Università degli Studi di Padova
Dipartimento di Ingegneria dell'Informazione

A thesis presented for Master's in ICT for Internet and Multimedia

Scheduling of Cellular Networks Working with Metasurfaces and Relays

Student:
Ali Amer Ali Algushti

Supervisor:
Prof. Stefano Tomasin

Matricola:
1225758

Academic year 2021/2022

ACKNOWLEDGEMENTS

I want to thank any person who played a vital role in my academic achievements. First, my family, who supported me throughout my master's degree and during the past years. Without them, I could never stand where I am today. Secondly, my brother Mohamed, who helped me during these 2 years and thanks to my extended family. Also, I would like to thank Federico Moretto who was ready to help whenever I had questions about my research. Thanks to anyone who provided me with useful advice whenever I needed. I want to express thankfulness to my research supervisor Prof. Tomasin who provided amazing guidance and I also would like to give special thanks to Prof. Jalal Srar and Prof. Omar Abu-Ella.

Thank you.

Contents

Abstract

Due to their ability to smartly reconfigure the transmission environment and wireless radio propagation of mm-wave broadcasts, Intelligent Reflective Surfaces (IRS's) have demonstrated they can resolve some of the concerns associated with mm-wave technology.

The IRS tunes the wireless environment to improve spectral and energy efficiency by combining a large number of low-cost, passively reflecting elements. By manipulating the frequency, amplitude, and phase of an incident wave, an IRS can then reflect the modified wave in the desired direction destination, avoiding the need for complicated signal processing.

RIS is an artificial surface that's electronically controlled by integrated electronics and made of electromagnetic (EM) material, also has special wireless communication capabilities. Current implementations incorporate traditional reflective arrays, LC (Liquid Crystal) surfaces, and software-defined meta-surfaces.

MM-Wave communications offer multi-gigabit wireless access due to their plentiful spectrum resources. Although it has high directivity and severe path loss, this technology is susceptible to blockage events, which can occur very frequently in dense urban environments. In order to overcome this issue, we introduced a new technology called an intelligent reflecting surface (IRS) that enables effective reflected paths to enhance mm-Wave signal coverage.

The optimal closed-form solution for the single IRS case can be derived by exploiting some key characteristics of mm-Wave channels, while a near-optimal analytical solution can be derived for the multi-IRS case. For both the single IRS case and the multi-IRS case, our analysis shows that the signal power receives increases quadratically with the number of reflecting elements. According to the results, IRSs can create effective virtual line-of-sight (LOS) paths, which, in turn, improves mm-Wave communication robustness to blockages.

Chapter 1

Introduction

IRS consists of a large number of passive reflection elements connected to a smart controller that can adjust the amplitude and phase of the incident signals in real-time to optimize the wireless channels between transmitters and receivers.
Because the reflection coefficients used in IRS are carefully chosen, the signals reflected can either be combined constructively with those from other paths to increase the desired signal strength at the receiver, or they can be combined destructively to reduce co-channel interference, thus providing a new degree of freedom for enhancing communications. Since IRSs are mostly passive devices that do not require active RF chains, they can be deployed densely in wireless networks at a low cost and with low power consumption.
In this thesis a wireless communication system is considered via a reconfigurable intelligent reflecting surface (IRS) that assists a transmitting source in communicating with a destination receiver. There will be a single antenna for all users (UEs), and transmissions will benefit from the IRS. There will be two cases: the first with only one IRS, and the second with two IRSs.
In both cases, we optimize power allocation, beamformers, and IRS configurations in order to maximize the achievable rate at the destination. The proposed approaches are compared with each other, i.e. with IRS, with two IRS's, and without IRS, and it is confirmed that a high capacity is achieved with two IRSs under optimal IRS configurations.
In the second chapter we will provide an overview of 5G technologies, then we will see a brief preview on the cell-free massive MIMO, and beamspace massive MIMO respectively,. In the third chapter we will discuss Intelligent Reflective Surfaces (IRS) and its concept, features, and implementations. In the fourth chapter we will see the system model and our scenarios.

Chapter 2

5G Technologies and Beyond

While the commercialization process for 5G communication networks under way, next-generation networks (6G) are studied to achieve faster and more reliable data transmission.
Intelligent reflective surfaces have recently received a great deal of interest in academic and industrial research. In November 2018, the Japanese mobile carrier NTT DoCoMo and a smart radar start-up Meta Wave demonstrated the application of meta-structure technology to data communication in the 28GHz band. The Intelligent Reflection Surface (IRS) consists of a large number of elements, each of which can independently reflects the incident signal.
The reflection may change the phase, the amplitude, the frequency, and even the polarization. So far, most studies have only considered the change as a phase shift in the incident signal so that the IRS does not consume transmit power. The main studies on IRSs and their architectures and functionalities are summarized in the Table 2.1 [1].
Intelligent reflective surface configure the wireless channel when the direct link in a bad condition, to improve the transmissions between both sides (sender and receiver). Fig. 4.1 illustrates IRS-assisted communications between a base station (BS) and user equipment (UE).
Using large arrays of antennas to significantly improve efficiency, the IRS concept is related to the technologies of massive MIMO. Therefore, we expect IRS to play a significant role in the development of 6G networks. IRS's differ from massive MIMO because IRS adjust wireless propagation environments to enhance communication.
In a massive-MIMO deployment, a logarithmic relationship between capacity and average transmit power exists instead of a linear relationship. As an alternative to massive MIMO, researchers have also compared and contrasted backscatter communications, millimeter-wave communication, and network densification with IRSs. In spite of this, these technologies typically consume a lot of

Examples of communications through IRSs			
References	Scheme	Architecture	Functionality
[2]	Intelligent wall	Active frequency selective surfaces with PIN diodes	Fully transparent reflecting surfaces
[3]	Spatial microwave modulators	Binary phase state tunable meta-surfaces	Shaping complex microwave fields
[4]	Coding meta-materials	Meta-surfaces with binary elements (0 or π phases)	Reconfigurable scattering patterns
[5]	Programmable meta-surface	Meta-surfaces with PIN diode-equipped cells	Reconfigurable phase, polarization, and scattering
[6]	Reconfigurable reflect-arrays	Reflect-arrays with tunable (varactor-tuned) resonators	Adjustable reflection phase
[7]	Large intelligent surface	Active contiguous surface for transmission and reception	Gains compared to massive MIMO
[8]	Software-controlled hypersurface	Meta-surfaces equipped with IoT gateways	Wave absorption, polarization, and steering

Table 2.1: Summarization the main studies in intelligent surfaces.

power and do not control the wireless environment.
As part of the intelligent reflecting surface (IRS) concept, electromagnetically controlled surfaces are applied to large-scale infrastructures such as building walls, airports, and stadiums. The large intelligent surface (LIS) can be active or partially passive and can have a large antenna spacing or continuous aperture.
The new technology also differs considerably from traditional MIMO systems in terms of transmission model and transceiver design. The purpose of this special issue is to highlight recent developments in multiple antenna technologies.
In this chapter we will provide an overview of 5G technologies.

2.1 5G Technologies:

In light of the need to deliver the required services in the wake of ever-increasing data rates and traffic volumes, the quest will continue. Technology for cellular networks has evolved from using fixed sector antennas to flexible multiple antenna solutions.
Third Generation Partnership Project (3GPP) released the first 5G New Radio (NR) release and the first commercial networks have already been launched. It is clear that massive MIMO technology, which consists of base stations with 1) at least 64 antennas and 2) an order of magnitude more antennas than the number of users equipment (UEs) is a key technology[9].
However, MIMO development is only at its beginning, and the end is not yet. We continue to have higher expectations of ubiquitous coverage and service quality as wireless connectivity becomes more crucial to our everyday lives. In addition to 5G, there are numerous future requirements not being met by the technology, including incredibly high bit rates, uniform performance across the coverage area, ultra-low latencies, great energy efficiency, and robustness against blocking and jamming. These requirements cannot be met easily.
The millimeter-wave (mm-Wave) frequency band is being strongly explored for use in 5G due to a large amount of unused bandwidth available in these frequency bands, which could result in higher bit rates. Mm-Wave communications have some fundamental disadvantages [10, 11].
Despite significant research efforts that have been made in this area over the past decade, the sensitivity to signal blockage has not been resolved. In mm-Wave bands, the shorter wavelengths lead to a shorter coherence time, so fewer data signals need to be multiplexed than in sub-6 GHz bands in order to acquire the same amount of channel state information (CSI).
It may not matter if mm-Wave can use 10 times more bandwidth, if only 10 times fewer data signals can be multiplexed, the bit rate might not increase. There is no doubt that problems increase in the sub-terahertz (THz) bands, above 0.1 THz, which is why they are being investigated beyond 5G.
In general, a multiple antenna algorithm is necessary for the sub-6 GHz spectrum as well as for frequencies higher than that. Such an algorithm must consider both frequency-division duplex (FDD) and time-division duplex (TDD) modes.
In light of modern multiple antenna technologies, and what we might be able to achieve beyond what is currently envisaged, it's time to look at what lies beyond 5G. For wireless network design beyond 5G, cell-free massive MIMO, beamspace massive MIMO, and intelligent reflecting surfaces (IRS) may all be potential paradigm shifts.

2.2 Massive MIMO:

Fifth-generation (5G) wireless communication networks, which were recently commercialized, achieved many improvements. These improvements included

air interface enhancements, spectrum expansions, and network intensifications based on a number of key technologies, such as massive multiple-input multiple-output (MIMO), millimeter-wave communications, and ultra-dense networks. Wireless communication has now reached the point where 5G is available commercially, but there are still many challenges to realizing connected intelligence and a range of applications such as industrial IoT, autonomy, brain-computer interfaces, digital twins, tactile Internet, etc. As a result, 6G wireless systems need to be researched as soon as possible.

2.2.1 Cell-Free Massive MIMO:

One of the candidate technologies for 6G wireless communication systems is cellular-free massive MIMO, which combines the advantages of distributed systems and massive MIMO to optimize wireless transmission efficiency. This technology is expected to be the international frontier in 6G wireless communications.
MIMO systems featuring distributed antenna systems (DAS) can cover dead spots and provide macro-diversity to improve the performance of cell-edge users[12]. The system provides better coverage and reduces system power consumption. Secondly, network (MIMO) and coordinated multi-point (CoMP) are two ways to reduce inter-cell interference by allowing neighboring access points (APs) to cooperate [13, 14].
To reduce data sharing, they divide the access points into disjoint clusters of cooperation. In contrast, interference between clusters is a serious problem, since inter-cellular interference cannot be removed within the cellular structure.
The interference between cells in the cellular paradigm cannot be removed. It was proposed that cell-free massive MIMO, which does not have cell or cellular boundaries, could be achieved by merging massive MIMO, DAS, and Network MIMO technologies.
The way this technology works can be described as follows: A MIMO network without cells consists of many access points serving a smaller number of users simultaneously and coherently on a single time-frequency resource[15].
APs can acquire CSI from uplink pilots between themselves and all UEs by operating in TDD mode and utilizing uplink-downlink channel reciprocity. Coherent transmission and reception are possible with this CSI, so only data signals must be shared between APs[16].
This information flow is enabled by the APs being connected via fronthaul to cloud-edge processors that handle the data encoding and decoding. The architecture is reminiscent of the cloud radio access network (C-RAN) architecture, which is also commonly called central processing units (CPUs) in the literature[17].
One can thus view C-RAN as an enabler of cell-free massive MIMO. Intel's CPUs usually only know the long-term channel characteristics, while the APs are the only ones with instantaneous channel status information. The basic

network architecture of a cell-free massive MIMO system is shown in Fig. 2.1.
The cell-free massive MIMO technology has been regarded as a crucial technol-

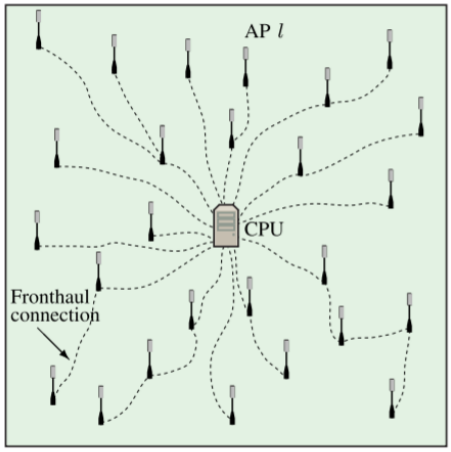

Figure 2.1: Illustration of the network architecture in cell-free massive MIMO.

ogy for the new sixth-generation (6G) networks due to its numerous advantages. Among its major benefits will be the ability to handle enormous quantities of data, to have ultra-low latency, to have high reliability, and to have ubiquitous and uniform coverage [18].

2.2.2 Beamspace Massive MIMO:

A MIMO transceivers with multiple antennas and higher carrier frequencies and bandwidth are more complex to implement. Utilizing the spatial structure of the channels and the transceiver hardware could reduce implementation complexity, but not at the expense of performance or operational flexibility.
A major component of hybrid beamforming and its future successors is beamspace massive MIMO, also known as beamspace massive MIMO.
In early radar systems, beamspace processing was an idea that was explored. Since the 1960s arrays with hundreds of elements have been a standard component of radar systems[19]. By using dual codebook precoding in LTE-Advanced (LTE-A), beamspace is widely utilized in cellular networks.
To adapt to the features of the channel, the matrix W_1, also known as the wideband matrix, was selected. Next, the matrix W_2, based on W_1, was selected. Transparency, as defined by LTE-A, became integral to virtualized channel pro-

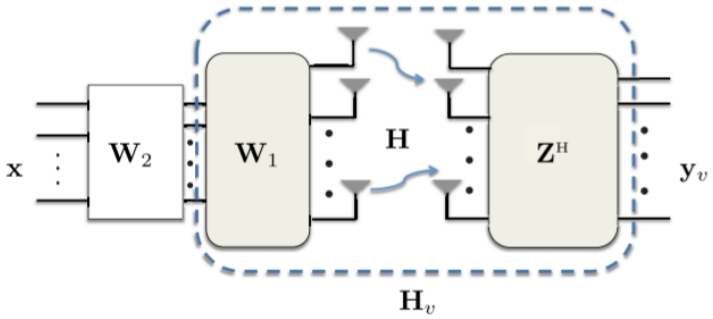

Figure 2.2: Illustration of the beamspace system model.

cessing.
Through CoMP systems, a UE can receive a signal sent from several geographically dispersed points, which are using different kinds of precoding techniques and multi-user transmission arrangements. By allowing the UE to be configured with multiple reference signals and CSI feedback reports, the standard simplifies the control, knowledge, and computational burden on the UE.
When beamspace formulation is used, beamspace signals can be used as K reference signals and CSI feedback reports as UE feedback. Reference signals could be sent over any of the possible first precoders, $W_1[1]$,..., $W_1[K]$. There is a virtual channel $H_v[k]$ for the precoder $W_1[k]$, and there is also virtual noise n_v equal to $(Z^H \cdot n)$ for the sounded precoder. In order to select a precoder for each virtual channel, the user would send feedback (via CSI feedback reports) for that selection[20].
Since the user does not need to know any $W_1[1]$,..., $W_1[K]$ techniques, operators and manufacturers can easily install and upgrade sophisticated precoding schemes. A user only needs to know how many reference signals have been received, the number of CSI feedback reports generated, and the corresponding configurations for each reference signal.
The 3GPP has been considering ways to make its technology future-proof for a variety of reasons. A recent increase in interest in hybrid beamforming and precoding at mm-Wave frequencies has reignited the practical use of beamspace[21]. Over the next few years, the size of commercial arrays will increase dramatically. It is common in the literature to discuss large-scale MIMO transmitters with hundreds of antennas, mm-Wave, and massive MIMO. Rethinking signal processing and implementing linear precoding is advantageous as the number of

antenna elements increases.
A beamspace MIMO formulation is the most popular approach. 5G and beyond systems will require beamspace notation, terminology, and thinking. There will be more antennas in the sub-6 GHz band.
Considering their dimensionality and unique hardware characteristics (hybrid analog-digital, sub-arrays, tiled arrays, etc.), sounding each array element will be next to impossible. In this regard, it will be best to implement MIMO processing using a virtual or effective channel approach. Beamspace will be essential at the same frequencies and higher than mm-Wave.
Large arrays using non-traditional array hardware may be used in these arrays. As beamspace becomes more important, optical-like thinking will become more prevalent.
The topic that we are interested in is the IRS and it is discussed in chapter III, after that, in chapter IV we will see the system model.

Chapter 3

Intelligent Reflective Surfaces

2D surface, composed of a large number of sub-wavelength reflecting elements (small antennas such as micro-strip patches). Reflective surfaces and their reflecting elements are commonly referred to as meta-surfaces where (Meta) is a Greek word means "beyond" and refers to the IRS's role beyond its normal function. IRS is aimed at enhancing the coverage of the BS by creating virtual links for users with blocked direct links.
In mm-Wave communications, which have a high blockage rate, this is particularly useful for coverage extension. In order to improve the desired signal power and suppress the interference at the cell edge, IRS can be deployed at the cell edge to improve signal attenuation from the serving cell and severe co-channel interference from neighboring cells.
In this chapter, we introduce the IRS concept and its features, the beamforming, the architecture of IRS, and how it works, and where we can use it, also, we will present another type of IRS that can be used in critical cases the Aerial Intelligent Reflecting Surface (AIRS).

3.1 Intelligent Reflecting Surface Concept:

Let's start with a standard surface with metal plates: when a signal is coming into the surface it will bounce off it in a direction determined by Snell's law, since it has a constant surface impedance.
The reconfigurable intelligent surface is built on a metasurface concept where we can alter the impedance along the surface. Thus, we can determine in which direction the incoming signal will bounce off, according to the generalized Snell's law. Fig. 3.1 illustrates metal plate where the surface impedance is constant and the ideal metasurface where we can altering surface impedance to phase-shift reflection.
We can't have a continuously variations in impedance but instead we will divide

the surface into small parts and each of them we have a constant value of this surface impedance.
By controlling that value we can select that a particular signal coming in from an angle will bounce off in another angle. IRSs were used in fixed reflect-arrays back in the 1960s.
Fig. 3.2 shows a reflect-arrays, where the signal is coming in and then it's gets focused on a particular point, so it is similar to satellite receiver but without a parabolic surface instead there is something that is flat and where it's divided into these different pieces which we control in such a way that the signal is getting focused on particular point.
In Fig. 3.3 where the RF transmitter sends a signal and the signal does not

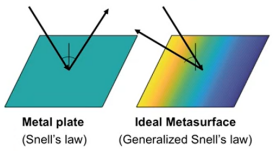

Figure 3.1: Metal plate and Ideal Metasurface.

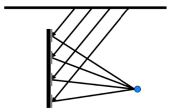

Figure 3.2: Reflect-Arrays.

reach the user (User 1) directly but it reaches the metasurface and we control it in such a way that the signal is reflected towards the user of interest, and then we can in real time change it. Instead of the previous user the signal will now be reflected towards another user (User 2) as shown in Fig. 3.4.
This is the main idea are reconfigurable intelligent surface that we're going to use them and put them out in the environment to improve the channel.

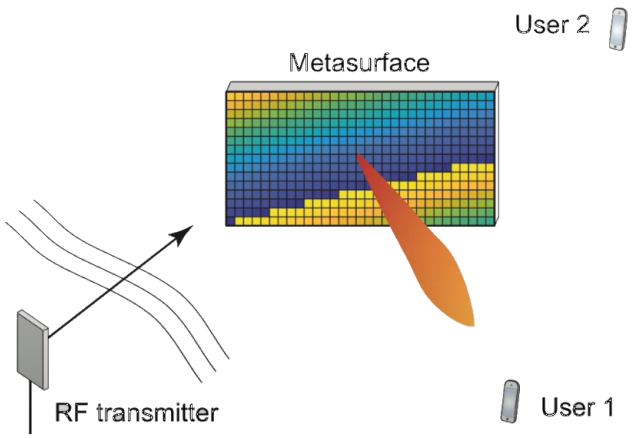

Figure 3.3: Real-time software-controlled Metasurface (The Signal Reflected Toward User 1).

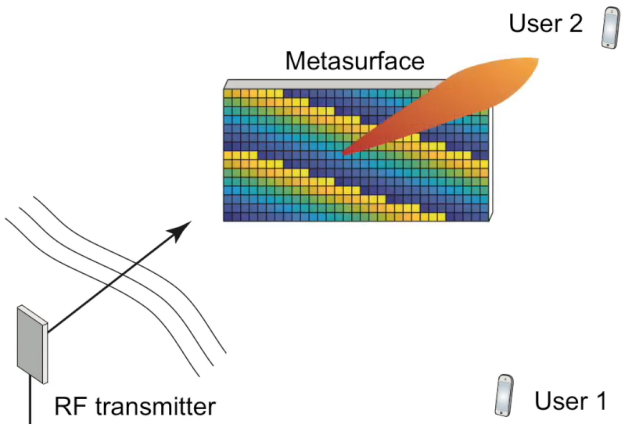

Figure 3.4: Real-time software-controlled Metasurface (The Signal Reflected Toward User 2).

This is an exciting idea from communication perspective because we can create intelligent propagation environments and from the set up in Fig. 3.5 we

have a source that's communicating with destination and the signal that goes directly between them is blocked and it's very weak.
The solution for this problem is to control what we do at the source, and control what we do at the destination, so we can try to encode the signal with the low coding rate and trying to do as much processing as possible at the receiver side to bring the signal back, but this is not the only solution because we can consider the metasurfaces and then we get an additional propagation path which is not direct, and we can control how the channel behaves.

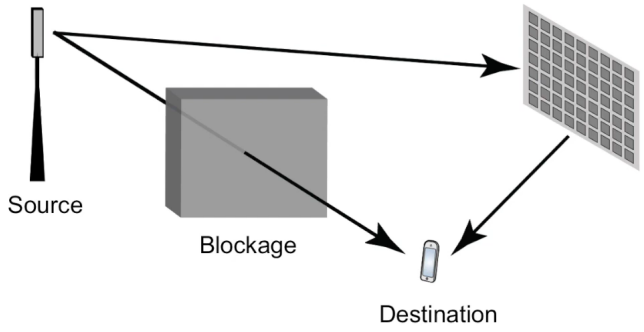

Figure 3.5: Intelligent Propagation Environment.

3.1.1 IRS Features:

The RIS technology consists of three fundamental characteristics, which we will describe one by one.

Creating Controllable Radio Environments:

IRS controls the way wireless signals are propagated between transmitters and receivers. Radio coding creates controllable, smart, and programmable environments, which can modify how signals travel from a transmitter to a receiver [22]. Utilizing channel state information (CSI), transmitters/receivers, and controllable entities within an environment can be optimized jointly.
A network architecture that utilizes diversity, beamforming, and multiplexing

to enhance the physical channel is referred to as cooperative communications. Controllable radio environments are defined as entities that are optimized with the transmitter and receiver.
A transparent relaying system and a regenerative relaying system are the two main categories. Those in the first category are relays that receive messages from the transmitter and process the signals in analog or digital form before re-radiating them to the receiver. An amplified signal is re-radiated by an amplifier in a way that can be transparent to the receiver in a classic protocol called "amplify-and-forward.". Amplification is all that is needed, with no baseband processing.
The relays decode and process the received signal in the digital baseband before re-transmitting the signal to the receiver in an optimized manner. The traditional relay operates in half-duplex, where reception and re-transmission take place in turns, but emerging regenerative full-duplex relays can receive and transmit simultaneously[23].
As a transparent relay, IRS offers a full-duplex protocol[24], so it operates in real-time, filling a void in the relaying taxonomy. By utilizing printed metamaterials, large surfaces can be implemented with reduced energy consumption and cost. As no amplifiers are needed, only power dissipation is needed in the hardware controlling reconfigurability[25].
A disadvantage of the device is the reduced signal range due to the lack of amplification[25]. In the absence of an IRS, it is possible that a multi-antenna Decode-and-Forward (DF) relays (a simple but sub-optimal relay scheme) will be used instead. IRS elements are presumed to have perfect CSI, and each IRS element scatters all incoming signal energy in a perfectly controlled phase[25]. There is no frequency dependence in the results, but the number of elements that fit on the surface grows quadratically with wavelength[25].
Decode-and-forward (DF) relays achieve much higher SNRs, but they also require a higher SNR to achieve the same degree of spectrum efficiency because they operate in half-duplex, whereas IRS relays do so in full-duplex[25].
Accordingly, IRS technology is able to control/optimize the propagation environment between the transmitter and receiver, just as previous relaying technologies have done. This technology is unique in that it reduces hardware complexity at the cost of increasing surface size[25].

Passive Beamforming:

The beamforming effect occurs when multiple antennas broadcast the same signal at different times. In locations where the copies are received simultaneously, there is constructive interference, and in places where they are received differently, there is destructive interference.
It would take N times more power for the receiver to receive the same amount of power if all power were transmitted by only one antenna, if the time delays between N transmit antennas are tuned for constructive interference.
Array gain shows the increasing spatial focusing of the beamformed signal with

increasing array size.
Passive beamforming is possible with an IRS. Surface area is proportional to the number of elements, N, which is proportional to the signal power it receives from the transmitter[25]. As with conventional beamforming, the array gain of N is obtained when the IRS transmits the signal with time delays selected to beamform at the receiver[25].
This combination results in an SNR at the receiver proportional to N^2 based on both of these effects which are proportional to N. It is known as the "square law"[26]. In general, gains of the kind described above only appear when the IRS (or transmitter array) has a small surface area compared to propagation distances. In order for the path loss (PL) to be approximately the same on all parts of the surface, the transmitter/receiver must be in the geometric far-field of the surface.
Due to the increasing surface area, the far-field approximation eventually breaks down as N increases. According to the law of conservation of energy, we can never receive more energy than we received. In this case, no asymptotic power scaling law can be applied linearly or quadratically[27].
When an IRS is used, the SNR achieved increases quadratically with an increasing number of elements for a number of realistically sized surfaces. A larger array of equal size should result in a better SNR when the IRS is set up this way. This issue is premised on the advantage of quadratic power scaling.
When the transmitter is in the far-field, the PL from each IRS element is immense, so it would be more accurate to say that the power loss between the transmitter and IRS decreases as $\frac{1}{N}$ [27].
If the IRS is replaced with an equal-size array of antennas transmitting with the same power as the IRS, the SNR cannot exceed the SNR achieved using the IRS, but the difference decreases as $\frac{1}{N}$.
For most SE values, the DF relay outperforms the RIS because of the power loss inherent in the "square law." Fig. 3.6 revisits the example in terms of end-to-end SNRs with the RIS versus the DF relay for different surface areas.

As the SNR gap narrows, the DF relay operation becomes the bottleneck, which is what caused the IRS to become more advantageous for high SEs[25]. This results in the IRS being able to passively beamform signals toward the receiver. Physically large surfaces are highly preferable because of the faster-than-linear SNR scaling[25].

Synthesizing A Different Surface Shape:

As well as forming beams, the IRS can simulate the scattering behavior of any arbitrary shaped surface. A diffusive scatterer can act as a superposition of beams or a scatterer for multiple beams[28].
An atypical mirror/reflector is a common example. Mirrors reflect plane waves as outgoing plane waves. This is called specular reflection. According to the law of reflection, a conventional mirror has the same angle of reflection to the

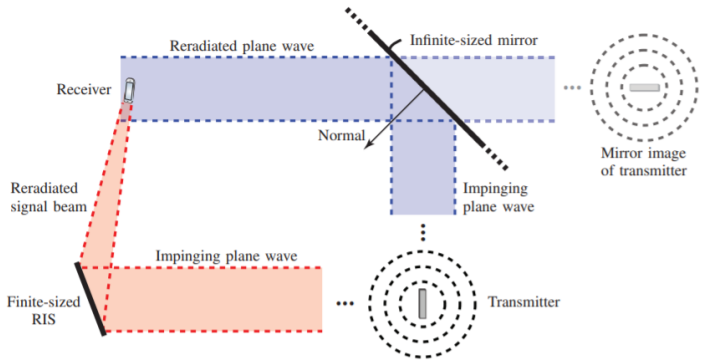

Figure 3.6: Comparing The End-to-End SNR Achieved by The RIS and The DF Relay.

surface normal as the angle of impingement, but on opposite sides[25].
Reflection of impinging plane waves by an anomalous mirror is at an "unnatural" angle to the normal surface image. An infinitely large homogeneous surface is the basis of conventional mirrors, and their apexes are naturally visible.
An anomalous mirror, by contrast, is artificially fabricated from an inhomogeneous surface and does not appear naturally. Mirrors have the characteristic of making the receiving source appear behind them to the receiver. Wave propagation can be analyzed as if the transmitter were moved to the mirror image[25].
IRSs are generally considered anomalous mirrors when their width or length are greater than 10 wavelengths[1]. When that is the case, the PL is the distance from the mirror image to the receiver added to the distance from the IRS to the receiver [1] which is the distance from the mirror image to the receiver.
Mirrors with zero beam-width reflect a signal perfectly. An IRS configured to focus a plane wave toward the far field will look like a plane wave when it is impinging on a finite-size IRS, but it will not be a plane wave. During beamforming from a far-field array, the beam width will be the same as that from a transmitter array of the same size.
For a surface that is 10 wavelengths in each dimension [25], the half-power beam width of the reflected signal becomes 6°. In practice, plane waves and mirrors are only approximate idealizations. Consequently, they can be used in geometrical optics to analyze imaging, since they are relatively accurate approximations in visible light.
Radio spectrum is an entirely different case. When it comes to radio signals, a surface that looks mirror-like to our eyes may not be one at all. A surface must

be 100,000 times larger in each dimension to identically reflect a signal [25] in the radio spectrum since the wavelength is roughly 100,000 times larger than in visible light.
Transmitters must have a distance of 100,000 times greater than their receivers to approximate spherical waves as plane waves, and receivers must have a distance of 100,000 times greater than the transmitter to perceive reflected waves as plane waves[25].
Since mirrors only exist at asymptotic limits, a finite-sized surface cannot always be approximated as a mirror. From a distance far enough from the IRS, its radiated field will have a beam-width that is inversely proportional to its size[25].
Due to the vast difference between the PL achieved by an equal-sized IRS, the claim that an anomaly mirror has the same path loss as an equal-sized IRS is a myth. The direction of a reflected signal can vary depending on the IRS[25].
The PL caused by an IRS should not be compared to the PL caused by an anomalous mirror[25]. Mirrors tend to behave like reflectors when they are close to the surface, but when they are far from it, they behave like diffusers.
The IRS can approximate the mirror response when the receiver is near the surface, but it would be less optimal; a mirror beam forms to points infinitely far away, whereas an IRS can focus on the actual receiver location.
The capability of an IRS to mimic the scattering of arbitrarily shaped objects of the same size[25] can be described as a parabolic reflector with curvature and direction that can be electronically steered. However, this is a simplification since an IRS is capable of mimicking the scattering of arbitrarily shaped objects of the same size[25].

3.1.2 Preliminaries - Passive Metallic Surface:

Suppose a rectangular, perfectly conducting plate $a \times b$, with a thickness of negligible amount is located in the horizontal plane (spanned by e_x and e_y), to illustrate the idea of a passive metallic surface scattered by an incident wave. An electromagnetic wave propagates from a distant point source, d_i, with a wave number $k = \frac{2*\pi}{\lambda}$, where * is the wavelength[29].
The polarization of the source assumes, for sake of argument, that the E-fields run parallel to e_x, and the H-fields lie in the plane spanned by e_y and e_z. Defining angle of incidence $\theta_i \in [0, \frac{\pi}{2}]$ as the angle between the wave's Poynting vector and e_z. Fig. 3.7 illustrates this setup[29].

The assumption is that d_i is sufficiently large in comparison to a and b (i.e., the source is in the far-field) so that the curvature of the wave-front, relative to the plate dimensions, can be neglected. As a result, the impinging wave-fields are approximated as a planar wave with an eigenvalue of some magnitude[29].
This approximation holds when the phase difference between the center and edges of the plate of a spherical wave is less than its plane wave approximation. Considering an angle of incidence of $\theta_i = 0$ in the center of the plate for the sake of argument; however, the analysis can be generalized to any angle of incidence.

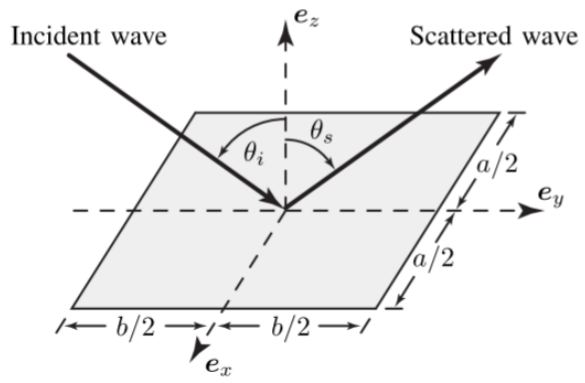

Figure 3.7: An Incident Wave is Scattered by Metal Plate.

If the wave is spherical, it has traveled $\sqrt{{d_i}^2 + \frac{b^2}{4}}$ from the source to the edges of the plate in the plane wave approximation. The phase difference follows:[29].

$$k\left(\sqrt{{d_i}^2 + \frac{b^2}{4}} - d_i\right) \approx \frac{\pi}{4}\frac{b^2}{\lambda d_i}$$

3.1.3 Joint Beamforming for IRS:

Joint beam-formation using statistical channel state information (CSI) is proposed for multiple-input multiple-output (MIMO) wireless communication using intelligent reflecting surfaces (IRS). A beamformer achieves maximum efficiency by maximizing both the IRS reflecting coefficients and the covariance matrices of the transmit symbol vector.
Based on the second-order momentum of the random channel matrices, the algorithm yields a general framework for evaluating ergodic rates without assuming any specific channel distributions. It is then validated by establishing practical channel correlation models[30].
By using the joint optimization algorithm, we find that the rate can be enlarged, but the gain over deploying the IRS elements randomly will depend heavily on the relative correlation distance and location of the IRS elements. IRS should, for example, be situated near either the transmitter or receiver and as a result. Putting IRS far from those positions would be counterproductive[30].

3.1.4 IRS's Enabled Cognitive Internet of Things:

A goal is to develop a cognitive internet of things (loT) that uses intelligent reflecting surfaces (IRSs). Due to the fact that secondary IoT devices share the spectrum with the primary network to transmit messages to the secondary access point (SAP), the secondary IoT devices cause interference to the primary access point (PAP) which profits from the interference power by charging the secondary devices[31].
By deploying IRSs between the IoT devices and SAP, we adopt a practical path loss model, in which each reflected signal is aligned to match its own desired direction. Further, two secondary network transmission policies are examined, one without/one with successive interference cancellation (SIC)[31].
To compensate for the near-far effect of IoT devices, signal-to-interference plus noise ratio balancing (SINR) is employed to distribute resources fairly among them. As a means of characterizing the interaction between primary and secondary networks, we propose a Stackelberg game strategy. To obtain the optimal power allocation and interference pricing for the proposed game, the Stackelberg equilibrium is derived analytically[31].

3.1.5 IRS Assisted Secret Key Generation:

It has emerged that intelligent reflecting surfaces (IRS) can help improve communication characteristics by making some adjustments. Generally, the phase, amplitude, frequency, or polarization of signals can be controlled smartly via IRS reflection coefficients[1].
Essentially, IRS is made up of many reconfigurable, passive reflectors, whose locations can also be adapted. Some of these IRS units can alter the incident signal on their own, which could enhance signal transmission. A growing number of studies have used IRSs to secure wireless communications at the physical layer.
This line of research suggests that the IRS can be used to improve secrecy data rates under wiretap channels, something called keyless information theory security.
When it comes to key generation for physical layer security technology, how to obtain more keys and utilize the channel state information (CSI) efficiently has always been a challenging issue. By using passive reflection, the IRS is capable of configuring the wireless channel in real-time, thereby enabling that channel to be improved in terms of encryption key capacity[32].
Using a three-node model and optimizing the placement of IRS units, it is possible to develop a scheme based on IRS-assisted key generation. Through the derivation of the key capacity expression of the IRS assisted system, further optimization of the placement and switching configuration of IRS units is achieved[32].
IRS units with limited resources can use this scheme to maximize the system's key capability. By optimizing the location of the IRS units, the simulation re-

sults show that the system can increase key capacity while also greatly reducing the bit inconsistency rate[32].
By leveraging channel probing, quantizing, information reconciliation, and privacy amplification, legitimate communication parties are able to glean the secure shared secrets. Fig. 3.8 shows the specific process for generating keys using CSI, and the steps are as follows.
A. Probing the channel occurs when the legitimate communication parties Alice and Bob send successive channel sounding signals and observe their channel characteristic values as they receive the signals[33].
B. The measurement quantization scheme is used by both parties to obtain the initial key by quantifying the channel features obtained by channel probing[34].
C. Reconciling the information: Noise, interferences, estimation errors, half-duplexes, etc., can cause missing bits in the initial key. During legitimate communication, the parties exchange information on the common channel to verify inconsistent key bits and obtain consistent key bits. Key sequence numbers, parity check matrices, etc., can be interactive information[35].
D. The eavesdropper Eve may overhear some information about the key during the channel probing and information reconciliation process, which poses a potential threat to the key's security. Using a publicly known set of universal hash functions, Alice and Bob can generate fixed-size output streams from large input streams, and this ensures that Eve will not discover the secret key[36].

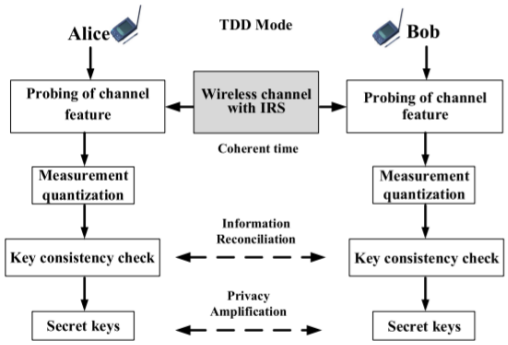

Figure 3.8: The Process of Secret Key Generation Based on Wireless Channel.

3.1.6 IRS's Persuasive Use Case:

In order for a new technology concept like IRS to move from theory to practice, considerable time and resources are required. It must be demonstrated that the improvements are 10 times greater than those of the existing technology [25].
It is not enough for us only to demonstrate 20 percent gains that could disappear in an imperfect implementation. We must demonstrate 10 times improvements with respect to a practical performance metric [25].
In the 5G development process, massive multiple-input multiple-output (MIMO) and mm-Wave communication passed the test since the former can serve up to 10 times as many concurrent users, and the latter, using much wider bandwidths, can increase the data rate for each user by 10 times [25]. Several other technologies that ran under the "5G" brand failed the test because their gains were insufficient. There are several technical features inherent to IRS technology that is not found in current mainstream tech [28].
For IRS technology to be developed, the critical question is: what is a compelling use case. There is no clear answer; IRS is like a hammer trying to find a nail. In the introduction, some IRS uses were listed, but does an IRS excel at anything. Extending coverage can be one of the solutions[25].
This configuration requirement further disadvantages IRS technology over wideband channels, because the IRS elements must be identical over the entire frequency band.
In addition, enhanced spatial multiplexing and interference mitigation could be a use case for this technology, but then it would need to beat cell-free massive MIMO, a technology that deploys distributed jointly operated antennas.
Maybe the most valuable application of IRS technology will be in the terahertz band, where coherent transceivers could be difficult to implement and weak channels still enable extra propagation paths to be useful. These are just speculations since there is no hard evidence yet [25].

3.1.7 Estimate Channels and Control an IRS in Real Time:

A proper configuration of CSI elements is crucial to IRS's envisioned use cases. IRS has two challenges when it comes to channel acquisition. To begin with, IRSs are not equipped with transceiver chains inherently, contrary to conventional transceiver architectures. It does not have any sensing capabilities; instead, it simply "reflects" the signals that are impinging upon it.
As a result, traditional channel estimation methods cannot be utilized. The introduction of an IRS into an existing configuration will increase channel coefficients in proportion to the number of elements. In order for IRS to be competitive, a large N is necessary; thus, the estimation overhead might be high.
So can an IRS be configured so that user mobility can be managed in real-time or not[25]. Several approaches have been proposed. In order to measure the received signal, a pilot sequence is repeatedly transmitted and measured while

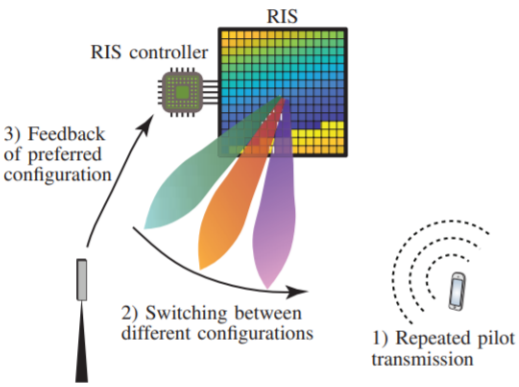

Figure 3.9: Approach: Configure the RIS to Transmit Pilots That The RIS Scatters Using Different Configurations.

using different IRS configurations. It can, for instance, turn on/off each element based on a pattern, or change the main reflection angle as the geometry changes[25]. To excite all the channel dimensions, N reconfigurations need to be tested at different times.
It is only possible to observe the channels to/from the IRS, and there is mutual coupling between the IRS elements that complicate the estimation. The IRS controller circuit and receiver require a wireless control loop between them with a capacity proportional to N and Fig. 3.9 illustrates it.[25].
The selection of appropriate time delays is computationally complex, even when CSI is acquired [37]. There is a possibility of grouping IRS elements into the same configuration[37] to reduce complexity, but this will result in performance losses.
By introducing receiver chains into the IRS, it facilitates sensing and channel estimation directly at the IRS, thus changing the passive nature of the IRS[38]. To estimate a wide-band channel from a few measurements, it needs to be spatially sparse and parametrized. A similar approach could be acceptable in mm-Wave or terahertz bands, but further work is needed on the channel and hardware modeling.
Channels can become flat as a result of sparseness over wide bandwidths. Algorithms based on learning and sparsity were analyzed in [38, 39]. It is still necessary to use a control loop to determine the configuration of the IRS and the beamforming at the transmitter/receiver, irrespective of whether the IRS

has sensing abilities.
Pilot overhead can be minimized by pulling advantages from special channel characteristics in estimation algorithms[40]. It is common for all users to use the semi-static channel between the BS and IRS, making the end-to-end channels correlated. A channel estimation algorithm is developed[40].
In the BS-to-IRS channel, many coefficients may be present if the BS has many antennas, but because this channel is semi-static, its coefficients are estimated less frequently compared to the IRS-to-user channel, which has fewer coefficients because users have fewer antennas[25].
The IRS can be used for fixed communication links, but when it comes to mobile communications, real-time channel parameters must be determined, regardless of where the communication takes place. A few millimeters of movement can change mm-Wave bands and above[25].
Whether any estimation protocol will be able to provide real-time reliability will have to be demonstrated, as well as which mobility conditions will be required. It is possible that IRS technology is more energy-efficient than alternative technologies [1], but this has not been quantified. The IRS will require a power source for reconfigurability and wireless control channels.
Because the control interface is expected to take the majority of the power at the IRS, the overall power consumption cannot be predicted until the channel estimates and reconfigurability have been solved.

3.1.8 Fundamentals of IRS's Architecture:

IRS architecture does not have a unified concept. Literature has proposed a variety of IRS designs with liquid crystals, micro-electromechanical systems, doped semiconductors, and electromechanical switches [41].
A typical architecture consists of at least three layers, including (1) a meta-atom layer, consisting of passive conductors and low-power active switches; (2) a control layer, which provides phase shift and amplitude adjustments; and (3) the communication layer, which provides communication between the control layer and the base station.
They can be reconfigured as electromagnetic scatterers at subwavelengths. This feature enables an IRS to be configured such that induced current patterns can be changed to generate a desired electromagnetic field response. Consequently, IRS can manage wavefronts in order to control steering, absorption, polarization, filtering, and collimation[42].

3.1.9 Liquid-Crystal-Loaded Metasurface:

In the proposed concept, the reflective phase of the metasurface can be electronically manipulated, enabling antenna beam steering. The liquid-crystal-tunable metasurface is made of a multilayered printed circuit board. Fig. 3.10 illustrates the configuration of the proposed metasurface made of high-impedance

material[43].
A solid ground plane is present at the bottom of the metasurface, while a gridded wire mesh is located on the top side for grounding microstrip patch tops. Microstrip patches are present in the middle layers. Microstrip patches are typically less than a quarter wavelength in size. Two microstrip patch layers are embedded with a liquid crystal mixture with a variable dielectric constant.
In this way, because of the anisotropy of the liquid crystal, the dielectric constant of the patches can be tuned depending on the electrostatic field between them. Therefore, adjusting the DC voltage at each cell individually we can electronically adjust the resonant frequency of each unit cell[43].
Because the frequency of the incoming wave in relation to the resonance frequency determines the reflection phase, such a surface can be adjusted to generate a distributed 2D phase shifter. As a result, an incoming wave can be redirected in a desired direction by altering the DC voltages of unit cells to give the desired reflected wave suitable phase distribution.

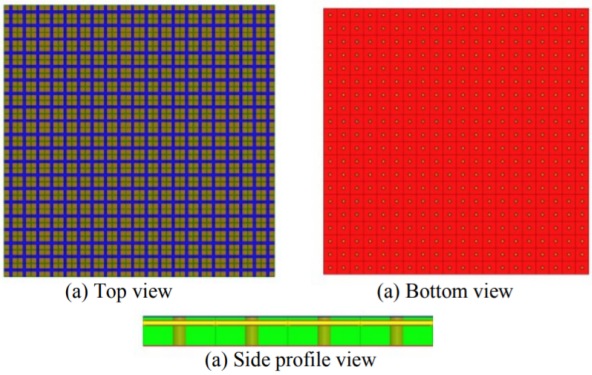

Figure 3.10: Liquid-Crystal-Tunable Metasurface.

3.1.10 State-of-The-Art Solutions:

RISs have been the subject of several studies and innovative solutions. To describe the RIS, many authors have used terms such as reconfigurable intelligent surfaces, large intelligent surfaces, intelligent reflecting surfaces, passive intelligent mirrors, artificial radio space, etc. This research was conducted on theoretical calculations of signal to noise ratio (SNR) and the symbol error probability (SEP), channel estimation, signal-to-interference ratio maximization, and joint

active and passive beamforming optimization.
A further feature of the study was the examination of the potential use of intelligent surfaces at millimeter-wave, Terahertz, and free-space optical communication systems, as well using the applications of machine learning tools, and physical layer security[1]. As a result, Table 3.1 describes the work relating to intelligent surfaces from a historical perspective[1].

3.1.11 Aerial Intelligent Reflecting Surface (AIRS):

Several research studies on IRS-aided communication have been conducted using terrestrial IRS that can be deployed, for example, on building facades or indoor walls/ceilings. However, such a deployment architecture shows several fundamental disadvantages.
On the deployment side, it is usually challenging to find a suitable location for IRS installation because of the cost of site rent, urban landscape, and whether the owner is willing to install large IRS on his properties.
Additionally, from the perspective of performance, buildings that have IRS mounted on facades or walls would generally only be able to serve nodes in half of the area, as illustrated in Fig. 3.11a. According to Fig. 3.12a, signal attenuation occurs in urban areas due to multiple reflections made by radio signals emanating from a source node. This results from the many reflections, which cause the signal attenuation to become more significant with each reflection[57].
In an aerial wireless network intelligent reflection maybe mounted on aerial platforms like balloons and unmanned aerial vehicles (UAVs).
An aerial IRS offers a number of advantages over terrestrial IRS. Because AIRS is elevated, it has a better chance of establishing line-of-sight (LoS) links with the ground nodes, which results in a better communication channel than terrestrial IRS.
Moreover, platforms can be positioned in flexible ways so that communication performance can be enhanced using 3D network design, thereby creating a new degree of freedom (DoF). A second capability of AIRS is its ability to provide panoramic/full-angle reflection, i.e., one AIRS can essentially assist in reflecting signals between any two nodes on the ground as shown in Fig. 3.11b[57].
Compared with a terrestrial IRS, which serves nodes in only half of the space, this is a huge benefit. As a result of its high likelihood of having Line-of-Sight (LoS) links with the ground nodes, AIRS can usually manipulate desired signals by one reflection only, even in complex urban environments as shown in Fig. 3.12b[57].

3.1.12 IRS Aided Communications:

Capacity/Data Rate Analyses of IRS-Aided Communications:

With IRS we have a linear relationship between average transmit power and capacity per square meter surface area rather than a logarithmic relationship

State-of-the-Art schemes with intelligent surfaces
A precoding-aided RIS scheme is considered for multi-user downlink transmission. Maximization of sum-rate and energy efficiency is performed with finite resolution reflectors[44, 45].
The problem of joint active and passive beamformer design is investigated for a MISO multi-user system. Minimization of the BS transmit power is performed through optimization and square-law scaling in transmit power is demonstrated[46, 47].
A mathematical framework is proposed for the calculation of the average SEP of RIS (LIS)-assisted systems. The concept of using the RIS as an AP (transmitter) is also introduced[48].
The concept of RIS (LIS)-assisted IM is proposed by considering the RIS as an AP. Greedy and maximum likelihood detectors are formulated for LIS-SM and LIS-SSK schemes along with theoretical derivations[48].
The maximization of the minimum SINR is investigated for an RIS-assisted multi-user MISO system. Rank-one and full-rank LOS channels, correlated RIS channels, and large-scale fading statistics are considered for phase optimization[49].
The problem of optimal transmit beamformer and RIS phase shifter is investigated to maximize the achievable spectral efficiency. It has been shown that the proposed algorithms guarantee locally optimal solutions[50].
An RIS-assisted large-scale MISO system is considered with Rician fading. Ergodic capacity of the system is maximized by the optimization of LIS phases[51].
A new channel estimation protocol for an RIS-assisted MISO system with energy harvesting is proposed. Active and passive near-optimal beamforming designs are formulated to enable efficient power transfer[52].
A new RIS architecture based on sparse channel sensors, in which some of the existing RIS units are active, is proposed. Two separate methods, based on compressive sensing and deep learning, are considered for the RIS design[53].
Considered the problem of cascaded channel estimation with fully passive RIS elements. An RIS-assisted massive multi-user MIMO system is considered and a three-stage channel estimation algorithm is proposed[54].
An RIS-assisted secure communication system with a legitimate receiver and an eavesdropper is considered. Showed that increasing the number of RIS reflecting elements is more beneficial than increasing the number of antenna elements at BS[55].
A downlink MISO broadcast system with multiple legitimate receivers and eavesdroppers is considered. A minimum-secrecy-rate maximization problem is formulated by jointly optimizing the BS beamformer and RIS reflecting coefficients[56].

Table 3.1: Summarization of the crucial contributions of the recent studies on state-of-the-art solutions based on intelligent surfaces.

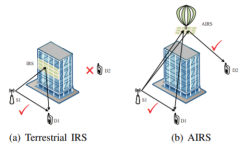

Figure 3.11: A terrestrial IRS's half-space reflection compared to an AIRS's panoramic/full-angle reflection.

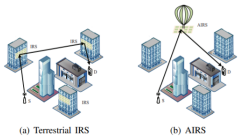

Figure 3.12: AIRS reduces reflections compared to a terrestrial IRS.

between average transmit power and capacity of massive MIMO[7].
According to the authors, radio frequency identification systems and single-antenna terminals are capable of communicating[58].

Power/Spectral Optimizations in IRS-Aided Communications:

In RIS, an incoming electromagnetic field can be altered in a customizable way using integrated electronic circuits. This architecture consists of one or a few layers of planar structures that can be easily made using lithography or nano printing.
It consists of reflect-arrays that use varactor diodes or other micro electro-mechanical systems that can be controlled electronically and whose resonant frequency is controlled electronically. On the incoming field, the RIS units can be positioned in discrete or continuous positions over the metasurface.
The less energy consumed by an IRS when compared to an amplifier-based relay transceiver is evident since it uses no amplifier. Furthermore, RIS structures have a very small hardware footprint, which makes them ideal for integration into communication environments, since they are easily reprogrammed.
As a result, they can be deployed in facades, rooms, factories, laptop cases, and even human clothing. Due to the fact that there is no amplifier in the RIS, it will achieve a lower gain than a traditional AF relay. Accordingly, a RIS-based system may not provide a more energy-efficient alternative to a traditional AF relay-based system[24].
The emergence of an innovative cost-effective technology capable of reconfiguring the wireless propagation environment can significantly enhance the spectrum and energy efficiency of wireless networks.An IRS functions as a metasurface composed of many passive reflecting elements, each of which has the ability to alter the phase shift of reflected signals independent of the others. Signal propagation can be adjusted adaptively at the receivers to combine signals constructively and reduce interference, which improves wireless performance.
An IRS-enabled wireless network with beamforming has recently drawn considerable attention. Using active beamforming at the BS and passive beamforming at the IRS, the problem of base station (BS) transmission power minimization has been addressed. A significant reduction in energy consumption in wireless

networks has been demonstrated by the IRS[24].
In the proposed IRS architecture, multiple users can be served simultaneously with a single BS using MISO model-assisted downlink, and beamforming and phase-shift matrices are optimized to minimize the total transmission power at the BS while simultaneously satisfying multiple users' quality-of-service (QoS)[24]. Alternative optimization methods to update the beamforming vectors and phase shift matrix alternately are presented here. These methods are discussed in the system model to solve the difficult non-convex bi-quadratic programming problem.

Channel Estimation for IRS-Aided Communications:

There is a large proportion of existing works which assume perfect channel state information (CSI) to design phase shifts at IRS and precoding vectors at BS. The IRS is not likely to be able to respond to this assumption in practice, given that the IRS has no radio resources of its own to send and receive pilot symbols, or signal processing capabilities to estimate channels. This is because the IRS has no radio resources to send and receive pilot symbols or signal processing capability to estimate channels. Due to these shortcomings, it is critical to reassess the potential benefits of IRS-assisted communication systems under an imperfect CSI model.
Due to the presence of CSI, it may be possible to use Zero-forcing (ZF) as a linear precoding method that is computationally simple and employ a decision feedback equalizer (DFE) structure to mitigate diffusive inter-symbol interference (ISI) and inter-link interference (ILI).
For an IRS-assisted single-user MISO system, one of the estimation techniques is Least Mean Squares (LMS) or Least Squares (LS), The IRS-assisted channels can be estimated one-by-one by keeping one IRS element active during each sub-phase of the channel estimation phase, and the remaining IRS elements off throughout the phase. An optimal solution to the IRS phase shift matrix could require all IRS elements to be active and reflecting throughout the estimation period.
For the channel estimation phase, the protocol assumes a noise-free environment at the BS, which definitely won't work in any real-world scenario. For the estimation of channels using compressive sensing and deep learning methods, only a few components of the IRS need to be active.

Deep Learning-Based Design for IRS-Aided Communications:

Configuring IRSs to facilitate wireless communication can benefit from deep learning. The IRS units are neurons, and their interactions with each other are the links, and the wireless propagation is seem as a deep neural network. The wireless network is trained using the data and learns how IRSs propagate and

configures them accordingly.
An IRS deep neural network learns the capabilities of wireless channels at all IRS units based on data from IRS units connected to the controller's baseband. To learn how the IRS should interact with incident signals, deep learning is used[59].

IRSs for Secure Communications:

Wireless communication has extensively investigated the security of the physical layer. Different techniques, such as jamming with artificial noise (AN) and using multiple antennas, can be used to boost secrecy communication rates.
Even with the aforementioned techniques, however, if the legitimate communication link and the spying link are spatially correlated in a high degree and the legitimate link has lower average power than the spying link as shown in Fig. 3.13, the achievable secrecy rate is not very high.

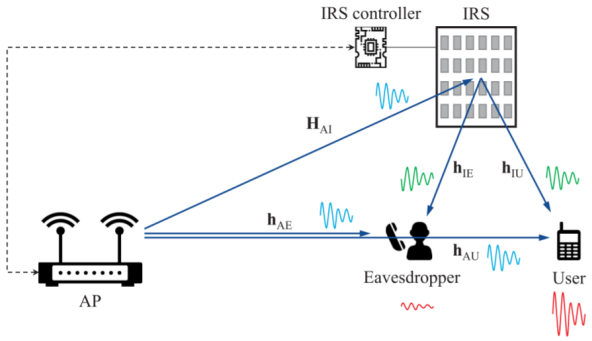

Figure 3.13: IRS-aided secure communication from an AP to a user in the presence of an eavesdropper.

Secure Wireless Communication via IRS:

Suppose there is a single-antenna eavesdropper in close proximity to a multi-antenna access point (AP), and the AP is configured to send secure communication to a user with a single antenna.
The IRS's reflecting units are first phase-shifted to boost the reflected signal's

strength and to cancel the reflected signal's strength, giving the user a high confidentiality rate.
The IRS's reflecting units are also phase-shifted so that the reflected signal is added constructively to the non-reflected signal at the user to enhance its power, as well as being destructively added to the eavesdropper's signal to cancel it, improving both user and eavesdropper privacy. It may also be possible to strike a balance between the power generated by the transmitter and that which reaches the IRS for signal enhancement/cancellation, respectively[60].
This means that the secrecy rate can be maximized by combining the active transmit beamforming at the AP and the passive reflects beamforming at the IRS[60].

IRSs for Terminal Positioning:

It is important to highlight some definitions before starting with the steps.
A.Fisher Information Matrix (FIM): is a way of measuring the amount of information that an observable random variable X carries about an unknown parameter θ of a distribution that models X. Formally, it is the variance of the score or the expected value of the observed information.
B.Cramer–Rao Lower Bound (CRLB): gives a lower estimate for the variance of an unbiased estimator. Estimators that are close to the CLRB are more unbiased (i.e. more preferable to use) than estimators further away.
Utilize IRS for terminal-positioning. Firstly, the Fisher Information Matrix (FIM) and the Cramer-Rao Lower Bound (CRLB) are derived in closed form for the purpose of positioning a terminal located perpendicular to the center of the IRS, which has been referred to as being on the Central Perpendicular Line (CPL) of the IRS[61].
There is no CPL terminal in which closed-form expressions of the CRLB are accessible, and alternatively, find approximate expressions that have been shown to be accurate. Under mild conditions, the surface area of the IRS decreases quadratically in all three Cartesian dimensions (x, y, and z). Analyzes the CRLB for positioning during the second step when the analog circuits of the IRS include an unknown phase ϕ [61].
The CRLBs then drastically degrade for all three dimensions, decreasing in exponential order in all three dimensions. Moreover, with an infinitely large IRS, the CRLB for the z-dimension with an unknown ϕ is 6 dB higher than the case without phase uncertainty, and the CRLB for estimating ϕ converges to a constant that depends on the wavelength λ[61].
The conclusion is that IRS can be distributed to expand its coverage and improve its overall performance [61]. The Fig.11 shows IRS-aided secure communication.

3.1.13 Large Intelligent Surface (LIS):

Wireless systems beyond 5G will be equipped with large intelligent surfaces (LIS's). The LIS concept involves stacking a massive number of radiating elements to realize an electromagnetically active surface. By reflecting incident signals, these elements can improve the coverage and rate of the wireless systems. Further motivation for the concept comes from the possibility of using fairly passive elements like analog phase shifters.
The use of wireless communication with LIS has gained increased attention in the past few years. Circuits for LIS can be realized with almost passive elements, configured via a reconfigurable parameter set [61].
There are a variety of candidates for designs, including conventional reflector arrays and software-defined meta materials. The LIS reconfigurable parameters have been optimized using several signal processing approaches (mainly considering the LIS as a reflecting surface) [61].
Multi-user downlink configuration using LIS with a single antenna is considered. In order to design these LIS phase matrices, computational low-complexity algorithms have been developed to model LIS elements as quantized phase shifters/reflectors [61].
LIS-assisted downlinks, similar to the previous one, have also been investigated, and both LIS reflection matrices and the base station precoder matrix have been designed taking into account the case when there is a line of sight (LOS) between the base station and the LIS.
The spectral efficiency of the system can be improved by combining LIS with index modulation. As a measure of the overall performance of the system, channel estimation errors were used to characterize data rates at an uplink multi-user scenario [62, 63].
The previous work [61, 62, 63] assumed that the channel information between the LIS and the transmitters/receivers was available at the base station, either perfectly or with errors.
The principal difficulty is that a large number of antennas (LIS elements) and the hardware constraints on these elements make obtaining channel knowledge one of the most challenging tasks for LIS systems. Specifically, there are two main approaches for designing the LIS reflection matrix when the LIS elements are implemented through phase shifters that simply reflect the incident signals. As a first step, it is normal to train all the LIS elements, normally one by one, before estimating the LIS-assisted channels at the transmitter/receiver, and then using those estimates to design the reflection matrix. Since the number of LIS elements is so large, this results in a massive channel training overhead. A quantized code-book can be utilized to select the LIS reflection matrix instead of explicit channel estimation.
Similar techniques are used in mm-Wave systems for beam training using phase shifter architectures [64, 65].
However, if one wishes to sufficiently quantify the space, the size of the reflection code-books must often exceed the number of antennas, and this leads to a substantial training overhead. In order to avoid this training overhead, it is

trivial to utilize fully-digital or hybrid analog/digital architectures at the LIS, where every antenna element is somehow connected to the baseband, from which channel estimation strategies can be applied [65, 66].
As a result of a large number of LIS elements, this approach is extremely complex and power-consuming. It is demonstrated that LIS-aided wireless communication systems can minimize the overhead of training by compressive sensing and deep learning, which is described as follows[47].
A novel architecture for LIS: introducing a design where all the elements are passive except for some randomly distributed active sensors.
In order to design an efficient LIS reflection matrix with low training overhead, only these few active sensors are connected to the controller's baseband.
LIS reflection matrix design using compressed sensing: Given the LIS architecture that has randomly distributed active elements, we propose a compressive sensing-based method to recover the full channel capacity between the LIS and transmitter/receiver from the sensed channel lengths from the few active elements. Building the LIS reflection matrices with no training overhead using the constructed channels.
The proposed solution can efficiently design the LIS reflection matrices when only a small fraction of the LIS elements are active yielding a promising solution for LIS systems from both energy efficiency and training overhead perspectives[47].
The proposed solution makes use of deep learning to design LIS reflection matrices that optimize the system's achievable rate. It does so by learning directly from sampled channels and by performing deep learning-based analysis of the LIS reflection matrices at the active LIS elements.
Based on the knowledge of the sampled channel vectors, the proposed approach allows the LIS system to interact with the incident signal and determine which environment descriptors are appropriate to use[47].
This means the LIS learns it should use this reflection matrix to reflect the incident signal when it observes these environment descriptors[47].
With the deep learning approach, rather than compressive sensing, prior observations at LIS are leveraged and no knowledge of the array structure is required.
DeepMIMO is a dataset that provides an accurate ray-tracing-based evaluation of the proposed solutions. This experiment showed that the developed compressive sensing and deep learning solutions are capable of approaching the ideal upper bound, which takes into account perfect channel knowledge and little training overhead with only a few LIS elements active. It shows potential solutions for LIS systems.
As illustrated in Fig. 3.14, the proposed LIS architecture is based on the random distribution of active channel sensors across the LIS. They operate in two ways, first as a channel sensing element that is connected to the baseband and uses a phase shift to reflect the incident signal, and secondly, as a reflective element that simply reflects the incident signal. Other LIS elements are passive reflectors and do not connect to the baseband.
Moreover, deep learning does not assume sparse channels and does not need any knowledge of LIS array geometry. This gain is only possible by collecting enough datasets for the deep learning model, which is not required for compres-

sive sensing.

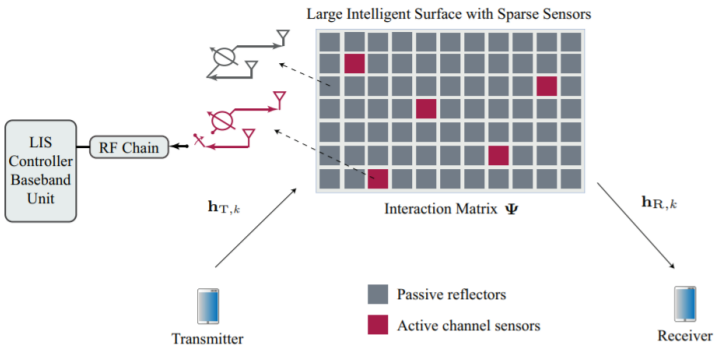

Figure 3.14: Large Intelligent Surface Architecture.

Chapter 4

Downlink Optimization with IRSs

In our system model will consider a (MISO) multiple-input single-output system that comprises a Uniform Linear Array (ULA) base station (BS) that transmits to a group $\mathcal{K}$ of K single-antenna UEs (User equipments). An intelligent reflective surface (IRS), having N elements is used to reflect the signal, as shown in Fig. 4.1.
The number of antennas at the BS is M. The BS transmits to only one UE in

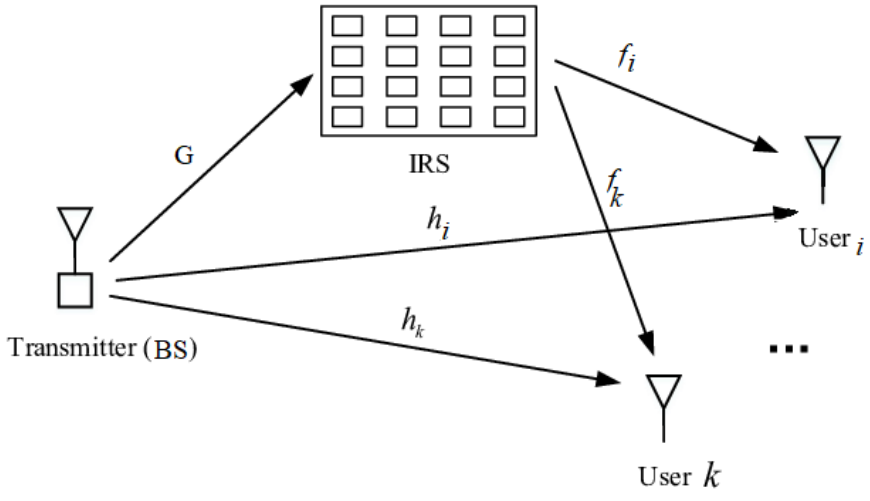

Figure 4.1: MISO System aided IRS.

every resource block (RB), by using an orthogonal frequency-division multiple-

access (OFDMA) scheme. We will suppose that the total system bandwidth split equally into C orthogonal subcarriers and F orthogonal RBs, indexed by $c \in \mathcal{C} = [0\ ;\ ...\ ;\ C\text{-}1]$ and $f \in \mathcal{F} = [0\ ;\ ...\ ;\ F\text{-}1]$, respectively. Also, the BS transmits the downlink signal to scheduled UE using transmit beamforming.
In this chapter, we will see the system model in detail. The downlink scenario and algorithms that will be used to optimize both the power and angles for the IRS. We will also implement 2 IRSs scenario and see the difference between it and the scenario with 1 IRS.

4.1 Channel Model

We consider two reference signals (RSs): the first is the channel state information RS (CSI-RS) and the other is the demodulation RS (DMRS). To estimate the CSI and calculate the channel quality indicator (CQI), we need to use both the CSI-RS and DMRS, which are beamformed RS. The IRS can't shift the phase of the incident wave during the CSI-RS period and, at the same time, a control signal will be sent from the BS to the IRS controller through an allocated control link during this period. After that, depending on the control signal the IRS reflects both the data signal and the DMRS with controlled phase shifts. The phase-shifted CSI will be estimated at the receiving UE (RUE) after receiving the DMRS, so we can finally decode the downlink signal.
The channel state is supposed to be a stationary stochastic process for each wireless link. The BS transmits the signal vector

$$\boldsymbol{x} = \sum_{k=1}^{K} \sqrt{p}_k \boldsymbol{w}_k s_k, \tag{4.1}$$

where for user k, p_k, $\boldsymbol{w}_k$, and s_k are the transmit power, the information symbol, and the beamforming vector respectively. Let $\boldsymbol{x}_k = \boldsymbol{w}_k\ s_k$, then the downlink received signal at UE k is obtained as

$$y_k = (\boldsymbol{h}_k^H + \boldsymbol{f}_k^H \boldsymbol{\Phi} \boldsymbol{G})\boldsymbol{x}_k + (\boldsymbol{h}_k^H + \boldsymbol{f}_k^H \boldsymbol{\Phi} \boldsymbol{G}) \sum_{i=1, i\neq k}^{K} \boldsymbol{x}_i + n_k, \tag{4.2}$$

where $\boldsymbol{h}_k \in \mathbb{C}^{M\times 1}$, $\boldsymbol{G} \in \mathbb{C}^{N\times M}$, and $\boldsymbol{f}_k \in \mathbb{C}^{N\times 1}$ are, respectively, the fading channels between the BS and DUE k, between the BS and RIS, and between RIS and RUE k. Note that, all channels, matrices, vectors, and signals presented in (3.2) should include the corresponding OFDM symbol index and the subcarrier index. However, for notational simplicity, we omit them here. The transmit beamforming vector $\boldsymbol{w}_k$ changes both the phase and amplitude of the effective downlink channel. The noise term is $n_k \sim \mathcal{CN}(0, \sigma^2)$.
The channel between the IRS and UE $\boldsymbol{f}_k$ and the channel between the BS and

UE $\boldsymbol{h}_k$ are defined as

$$[\boldsymbol{f}_k]_n = \sum_{\ell=1}^{L} \sqrt{\beta_{k,\ell}^{(f)}}\, e^{j\frac{2\pi}{\lambda}[(n-1)d_{IRS}\sin\theta_{k,\ell}\sin\phi_{k,\ell}]}, \tag{4.3}$$

$$[\boldsymbol{h}_k]_m = \sum_{\ell=1}^{L} \sqrt{\beta_{k,\ell}^{(h)}}\, e^{j\frac{2\pi}{\lambda}[(m-1)d_{BS}\sin\theta'_{k,\ell}\sin\phi'_{k,\ell}]}, \tag{4.4}$$

$m = 1,..., M$, $n = 1,...,N$, where λ is the wavelength (the light of speed divided by the frequency $\lambda = \frac{c}{f}$) , $\theta_{k,\ell}$ and $\phi_{k,\ell}$ represent the elevation and azimuth LoS angles of departure (AoD) respectively at the BS w.r.t the IRS element, and $\theta_{k,\ell}$ and $\phi_{k,\ell}$ represent the elevation and azimuth LoS angles of arrival (AoA) respectively at the IRS, where the azimuth angles are independent uniform random variables from $-\pi$ to π and elevation angles are independent uniform random variables from $-\pi/2$ to $\pi/2$. Moreover $\beta_{k,\ell}$ is the channel fading gain for the BS-to-IRS link, follows an exponential distribution whose overall is decreasing with the distance. Since we have 3 paths consider the first path is the shortest one, then the second, and the third path respectively,. d_{BS} is the inter-antenna separation at the BS and d_{IRS} is the inter-element separation at the IRS. Let us define

$$\boldsymbol{H} = [\boldsymbol{h}_1^H, ..., \boldsymbol{h}_K^H] \in \mathbb{C}^{K\times M}$$

and

$$\boldsymbol{F} = [\boldsymbol{f}_1^H, ..., \boldsymbol{f}_K^H] \in \mathbb{C}^{K\times N}$$

The reflection matrix $\boldsymbol{\Phi} \in \mathbb{C}^{N\times N}$ (operating as a passive beamformer) is controlled by the IRS control signal from the BS, and includes the reflection amplitudes and phases resulting from N reflecting elements i.e.,

$$\boldsymbol{\Phi} = diag(A(\angle\Gamma_1)e^{j\angle\Gamma_1}, A(\angle\Gamma_2)e^{j\angle\Gamma_2}, ..., A(\angle\Gamma_N)e^{j\angle\Gamma_N}), \tag{4.5}$$

where $A(\angle\Gamma_n) \in [0, 1]$ and $\angle\Gamma_n \in [0, 2\pi]$ are the reflection amplitude and phase at reflecting element n of the RIS, respectively.
We consider a practical reflection power loss resulting from the power consumption at the resistance of the reflecting circuit. The relation between a reflection amplitude and its phase is approximated under this practical reflection power loss as follows

$$A(\angle\Gamma_n) = (1 - |\Gamma|_{min}) \left[\frac{\sin(\angle\Gamma_n - 0.43\pi) + 1}{2}\right]^{1.6} + |\Gamma|_{min}, \tag{4.6}$$

where $|\Gamma|_{min} = 0.2$ is the minimum reflection amplitude[67]. The instantaneous SNR at UE k is

$$\gamma_k = \frac{p_k|(\boldsymbol{h}_k^H + \boldsymbol{f}_k^H\boldsymbol{\Phi}\boldsymbol{G})\boldsymbol{w}_k|^2}{\sigma^2}. \tag{4.7}$$

The BS-to-IRS mm-Wave channel matrix $\boldsymbol{G}$ can be generated as:

$$[\boldsymbol{G}]_{M,m} = \sum_{\ell=1}^{L} \sqrt{\beta_\ell^{(G)}}\, e^{j\frac{2\pi}{\lambda}[(m-1)d_{BS}\sin\theta''_{\ell,1}\sin\phi''_{\ell,1} + (n-1)d_{IRS}\sin\theta''_{\ell,2}\sin\phi''_{\ell,2}]}, \tag{4.8}$$

where L is the number of paths, and $\theta''_{\ell,1}$, $\theta''_{\ell,2}$, and $\phi''_{\ell,1}$, $\phi''_{\ell,2}$ are elevation and azimuth angles, and as the same as $\theta_{k,\ell}$ and $\phi_{k,\ell}$ they are independent uniform random variables. $\beta_\ell^{(G)}$ is the path loss and defined as an exponential distribution.

4.2 Maximizing The Capacity For A Single User

We jointly optimize the (active) transmit beamforming at the BS and the (passive) phase shifters at the IRS to maximize the SNR at the user.
The corresponding optimization problem can be formulated as

$$(P1): \max_{\boldsymbol{w}_k, \{\angle\Gamma_n\}} \quad \left|(\boldsymbol{h}_k^H + \boldsymbol{f}_k^H \boldsymbol{\Phi} \boldsymbol{G})\boldsymbol{w}_k\right|^2 \tag{4.9}$$

$$\text{s.t.} \quad \|\boldsymbol{w}_k\|^2 \leq P_t \tag{4.10}$$

$$0 \leq \angle\Gamma_n \leq 2\pi, \forall n = 1, ..., N. \tag{4.11}$$

4.3 Maximizing The Capacity For Multiple Users

In MU-MIMO systems, the inter user interference (IUI) is the most serious problem that affects the signal detection at the receiver and the Signal to Interference plus Noise Ratio (SINR) at UE k is

$$\gamma_k = \frac{p_k|(\boldsymbol{h}_k^H + \boldsymbol{f}_k^H \boldsymbol{\Phi} \boldsymbol{G})\boldsymbol{w}_k|^2}{\sum_{i=1, i\neq k}^{K} p_i|(\boldsymbol{h}_k^H + \boldsymbol{f}_k^H \boldsymbol{\Phi} \boldsymbol{G})\boldsymbol{w}_i|^2 + \sigma^2}. \tag{4.12}$$

Thus, the most important objective is to cancel the IUI utilizing more advanced algorithms for data detection in uplink and precoding in the downlink. The signal received by all the users is

$$\boldsymbol{y} = [\boldsymbol{y}_1, ..., \boldsymbol{y}_K]^T = (\boldsymbol{H} + \boldsymbol{F}\boldsymbol{\Phi}\boldsymbol{G}^H)\,\boldsymbol{W}\,\boldsymbol{s} + \boldsymbol{n}_k, \tag{4.13}$$

where $\boldsymbol{W} = [\boldsymbol{w}_1, ..., \boldsymbol{w}_K] \in \mathbb{C}^{M\times K}$, and $\boldsymbol{s} = [\boldsymbol{s}_1, ..., \boldsymbol{s}_K]^T$. We can also define

$$\boldsymbol{H}_t = \boldsymbol{H} + \boldsymbol{F}\boldsymbol{\Phi}\boldsymbol{G}^H. \tag{4.14}$$

4.3.1 Downlink Scenario

In the downlink transmission, to facilitate and make the detection less complex at the receiver side, a pre-processing (precoding) is made at the BS where a multi-antenna transmitter can communicate simultaneously with single or multiple antenna users. In the downlink, we consider the ZF precoding. By defining

$$\boldsymbol{W} = \boldsymbol{H}_t^H(\boldsymbol{H}_t\boldsymbol{H}_t^H)^{-1}, \tag{4.15}$$

We normalize $\boldsymbol{W}$ and obtain the ZF precoder

$$\boldsymbol{W}'_{*,k} = \frac{\boldsymbol{W}_{*,k}}{\left\| \boldsymbol{W}_{*,k} \right\|}. \tag{4.16}$$

Hence we have

$$\boldsymbol{D} = \boldsymbol{H}_t \boldsymbol{W}', \tag{4.17}$$

Where $\boldsymbol{D}$ is diagonal with entries $d_k = \frac{1}{\left\| \boldsymbol{W}_{*,k} \right\|}$, $k = 1,..., K$ and $y_k{=}d_k\ s_k + n_k$. Then, the optimization problem to maximize the sum rate can be written as

$$\max_{p_k, \boldsymbol{\Phi}} \quad \sum_{k=1}^{K} \log_2(1 + \frac{p_k d_k}{\sigma^2}), \tag{4.18}$$

$$\text{s.t.} \quad |v_n| \leq 1, \forall n = 1, ..., N, \tag{4.19}$$

$$\sum_{k=1}^{K} p_k \leq P_t \quad . \tag{4.20}$$

4.3.2 Optimizing Power

The maximization of concave function is equal to the minimization of convex function so we will work on it as it is and formulate the Lagrangian function (Water-filling Algorithm) as shown in the example in Fig. 4.2.
Primal problem:

$$\mathscr{L}(p_k, \lambda_k, \mu) = \sum_{k=1}^{K} \log_2(1 + p_k d_k) - \sum_{k=1}^{K} \lambda_k p_k - \mu \sum_{k=1}^{K} (p_k - P_t). \tag{4.21}$$

Dual problem: Minimizing the Lagrangian dual function, which is a function of only the Lagrangian multipliers and can be formulated as

$$(P) : \min_{\lambda} g(\lambda_k, \mu) \tag{4.22}$$

$$\lambda_k \geq 0, k = 1, ..., K, \quad . \tag{4.23}$$

The Lagrangian dual function g is the supremum over the p_k's on the Lagrangian function $\mathscr{L}(p_k, \lambda, \mu)$ (the optimal power expression), i.e.,

$$g(\lambda_k, \mu) = \sup_{p_k} \mathscr{L}(p_k, \lambda_k, \mu). \tag{4.24}$$

To find the supremum we will derive with the respect to each p_k.

$$\frac{\partial \mathscr{L}}{\partial p_k} = \frac{d_k}{1 + p_k d_k} - \lambda_k - \mu = 0, \tag{4.25}$$

$$p_k = \frac{1}{\lambda_k + \mu} - \frac{1}{d_k}. \tag{4.26}$$

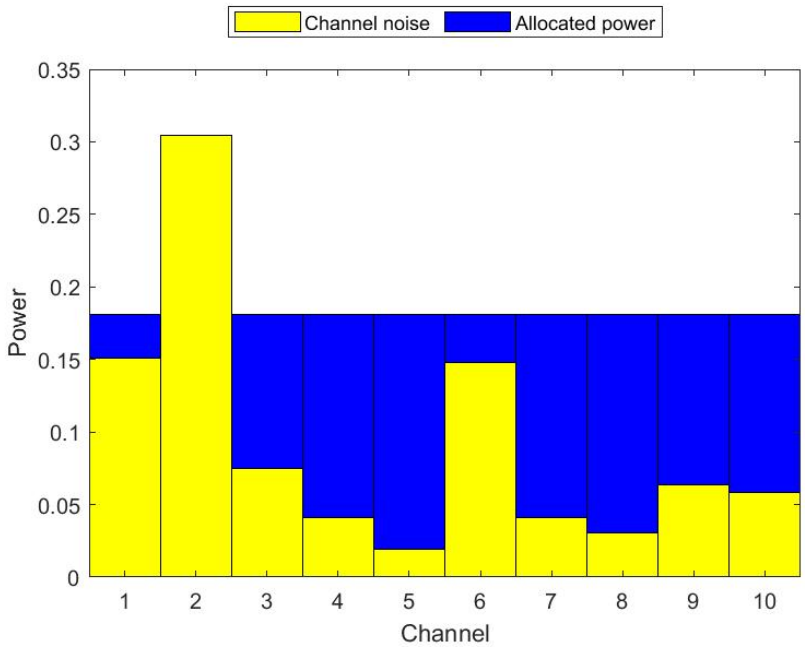

Figure 4.2: Water-filling Algorithm.

Now, p_k is always positive, so the term $\left(\frac{1}{\lambda_k+\mu} - \frac{1}{d_k}\right)^+$ should be positive. where $p_k^{+\cdot} = max(p_k, 0)$. by forcing p_k to be positive the constraint $p_k \geq 0$ is not important. In this case λ_k either if it is a positive number or zero p_k is always positive.
From (4.25) and (4.26) we have

$$\mathscr{L}(p_k, \lambda_k, \mu) = \sum_{k=1}^{K} \log_2(1 + p_k d_k) - \mu[\sum_{k=1}^{K}(p_k - P_t)], \tag{4.27}$$

$$p_k^* = \left(\frac{1}{\mu} - \frac{1}{d_k}\right)^+, \tag{4.28}$$

Where ${p_k}^*$ is the optimal power. By plugging (4.28) into (4.24) the Lagrangian dual function can be formulated as

$$g(\mu) = \mathscr{L}(p_k^*, \mu) = \sum_{k=1}^{K} \log_2(1 + p_k^* d_k) - \mu[\sum_{k=1}^{K}({p_k}^* - P_t)] \tag{4.29}$$

$$\min_{\mu} g(\mu) = \sum_{k=1}^{K} \log_2(1 + \left(\frac{1}{\mu} - \frac{1}{d_k}\right)^+ d_k - \mu[\sum_{k=1}^{K}\left(\frac{1}{\mu} - \frac{1}{d_k}\right)^+ - P_t)], \tag{4.30}$$

$$\frac{1}{\mu^*} = p_k^* + \frac{1}{d_k} \tag{4.31}$$

Where μ^* is the optimal solution and by plugging in (4.28), we have

$$p_k{}^* = \begin{cases} \frac{1}{\mu^*} - \frac{1}{d_k}, & \text{if } \frac{1}{\mu^*} \geq \frac{1}{d_k}. \\ 0, & \text{if } \frac{1}{\mu^*} < \frac{1}{d_k}. \end{cases} \tag{4.32}$$

4.3.3 Reflection Phase Selection Algorithms

Algorithm 1 (Genetic Algorithm)

First, we have to highlight the definition for some terms that we will use to describe the genetic algorithm (GA).
A. Population : a subset that contains all the possible solutions that can solve a problem.
B. Chromosomes : one of the solutions in the population.
C. Fitness Function : a function that uses a particular input to create a progressed output. The solution is utilized as the input whereas the output is in the form of a reasonable solution.
It is one of the random-based evolutionary algorithms, and a simple type of it is a GA. Is used primarily to identify the optimal parameters (solutions) for computational problems. We set up the algorithm to find random members by mutation and crossover (based on stochastic, the population), so we can choose the level of control and randomization using our optimization technique[68].
If we compare the random search and exhaustive search with the GA we can say that this algorithm is more efficient.
GA can give results to problems that other optimization methods cannot give and can not even deal with that kind of problem. The optimization variables $\boldsymbol{W}$ and $\boldsymbol{\Phi}$ are deeply coupled in the non-convex objective function and that is because, in our scenario, the phase optimization problem is overall indeed harder than the power minimization problem.
First, the reflection amplitude is always 1. This algorithm finds a local unconstrained minimum, for a given objective function. The function that we are using in this algorithm is the total capacity after zero forcing and water filling. We will modify this Algorithm to find the maximum instead of the minimum to meet our consideration of finding the optimal phases which will maximize the network sum rate.
GA is started by making a population of chromosomes employing an irregular number generator, so our population will form in a matrix, each row represents a chromosome in this matrix. The fitness of every member of each of the population is at that point assessed through the cost function, and depending on the environment this cost function works. weights the significance of each quality for survivability in a specific environment is will be done also by the cost function.
Each adjustment esteem is weighted agreeing to how likely that characteristic

will result in chromosome 1) mating or 2) being eaten by a predator. To judge the versatility of each chromosome the last step that should be done is composing a cost function that duplicates the versatility values for the chromosome by the environment weights. The GA schedule is arranged to search for minima and because of that, the negative sign is connected to the cost function.
The algorithm is attempting to optimize what we called the fitness function. We used the word "fitness" which is originally from evolutionary theory. since the fitness function tests and measures how 'fit' each potential result is, this is why we utilize it. The fitness function is one of the foremost urgent parts of the algorithm, it can cruel the distinction between finding the ideal solution and finding no solution at all because it is the as it stepped within the algorithm that decides how the chromosomes will alter over time.
The population's evolution will "ruthlessly exploit" all "boundary conditions" and inconspicuous abscond within the fitness function, and the only way to identify this can be by fair running the algorithm and looking at the chromosomes that result. chromosome: it should accurately score the chromosomes based on an extended fitness value so that a somewhat complete solution can be recognized from a more total solution, and not only know what is a good or bad chromosome.

Algorithm 2 (Alternating Beamforming with Intelligent Reflecting Surface Element Allocation)

In this algorithm, we designate each IRS component independently to each user, hence, within the beamforming stage we consider a single user at a time.
A. IRS Element Allocation: The proposed IRS component allocation is based on the key thought of coordinating one IRS component to one UE to diminish complexity. In any case, this concept ought to be more indicated with two factors: 1) the number of IRS elements each UE should be assigned to, and 2) the selection of specific IRS elements each UE should be allocated with. These factors depend on our primary objective, i.e., maximizing the minimum rate. To accomplish this objective, we relegate more IRS components to the powerless UEs. The steps (1-16) that define algorithm 2 are shown in Table 4.1[69].
B. Alternating Beamforming Technique: In this technique we will transmit beamformer at the BS and update the IRS phases, but with another step of IRS element allocation. The proposed substituting beamforming method, in any way, does not depend on any complex optimization operation, and it is immensely diminishing the complexity compared to the GA[69].
We will use familiar transmit beamformers like the zero-forcing (ZF) beamformer or as an alternative, it could be used the maximum ratio transmission (MRT) beamformer. Through the fact that each IRS element considers only one UE, each IRS element phase update can be expressed in closed form as in (4.33). Hence, by coherently combining the signal to a particular UE instead of jointly considering all UEs, the phase which updated can be computed with

Algorithm 2 (Pseudo-code for IRS allocation and alternating beamforming)

Initialization : *Random* $\boldsymbol{\Phi}$, $\boldsymbol{W}, \mathcal{N}_0 = \{1, 2, ..., N\}, \mathcal{N}_k = \phi, 1 \leq k \leq K$

repeat

With $\alpha_k = \frac{1}{\left|\boldsymbol{h}_{d,k}^H \boldsymbol{w}_k\right|}$, *set* $\ell_k = [N \frac{\alpha_k}{\sum_{i=1}^{K} \alpha_i}]$ *with remainders as equation* (6) *in* [68]

Order UEs as $\alpha_{m_1} \geq \alpha_{m_2} \geq ... \geq \alpha_{m_K}$

for $V = 1$ **to** K **do**

repeat

$n_0 = argmax_n \left| f_{n,m_i}^* \boldsymbol{g}_n^H \boldsymbol{w}_{m_i} \right|, n \in \mathcal{N}_0$

$\mathcal{N}_{m_i} = \mathcal{N}_{m_i} + \{n_0\},\ \mathcal{N}_0 = \mathcal{N}_0 - \{n_0\}$

until *Iteration is repeated* ℓ_{m_i} *number of times*

for $k = 1$ **to** K **do**

repeat

$\angle\theta_{n_k} = -\angle(\boldsymbol{h}_{d,k}^H \boldsymbol{w}_k) - \angle f_{n_k,k} + \angle(\boldsymbol{g}_{n,k}^H \boldsymbol{w}_k)$

$\mathcal{N}_k = \mathcal{N}_k - \{n_k\},\ \mathcal{N}_0 = \mathcal{N}_0 + \{n_k\}$

until $\mathcal{N}_k = \phi$

Update transmit beamformer $\boldsymbol{W}$ *using effective channel formed by* $\boldsymbol{\Phi}$

until *Iteration is repeated* $V > 0$ *number of times*

Table 4.1: The steps of Algorithm 2

negligible complexity.

$$\angle\theta_n^{(v+1)} = -\angle(\boldsymbol{h}_{d,k}^H \boldsymbol{w}_k^{(v)}) - \angle f_{n,k} + \angle(g_n^H \boldsymbol{w}_k^{(v)}),\ n \in \mathcal{N}_k \tag{4.33}$$

C. Rationale of The Proposed Alternating Beamforming: The effective channel is the conventional downlink channel. As the transmit beamformer and IRS stages are updated, the IRS stage update will modify the effective channel, and because of that will make the past transmit beamformer unsuitable to the new effective channel.
We'll utilize a ZF beamformer and after that we will update the transmit beam-

former as follows,

$$\begin{aligned} \boldsymbol{h}_{eff,k}^{(v)} &= \boldsymbol{h}_{d,k} + \boldsymbol{G}\boldsymbol{\Phi}^{(v)} f_k, \\ \boldsymbol{w}_k^{(v)} &= (\boldsymbol{h}_{eff,k}^{(v)}{}^H \boldsymbol{h}_{eff,k}^{(v)})^{-1} \boldsymbol{h}_{eff,k}^{(v)}{}^H, \end{aligned} \tag{4.34}$$

It is highly likely that $\boldsymbol{W}^{(v-1)}$ is outdated for $\boldsymbol{h}_{eff,k}^{v}$ because of the number v-th of IRS phase update. So, by updating the transmit beamformer, with a high probability the performance, in this case, the min-rate, would increase.
In the stage of allocating the IRS, elements will be allocated to the UEs according to Section A. The beamforming gain of the UEs and the transmit beamformer will be updated.
As a result of updating the IRS element allocation, the number of IRS elements will be newly assigned followed by newly allocating the IRS elements. This level will prohibit the situation of allocating insufficient IRS elements during iterations or strengthening wrong UEs.
D. The Complexity and The Outline of The Proposed Beamforming Technique: The overall proposed alternating beamforming technique is summarized in Algorithm 2 where $\mathcal{N}_0$ is the group of unassigned IRS elements. First, with the transmit beamformer fixed, allocate the IRS elements to the UEs. After that, by using the following equations

$$\begin{aligned} r &= N - \sum_{k=1}^{K} \ell_k, \\ \ell_{k_0} &= \ell_{k_0} + r,\ k_0 = \underset{k}{\operatorname{argmax}}\ \alpha_k \end{aligned} \tag{4.35}$$

$$\left| \boldsymbol{h}_{d,k}^H \boldsymbol{w}_k^{(v)} + \sum_{n=1}^{N} f_{n,k}^* (\phi_n^{(v)})^* \boldsymbol{g}_n^H \boldsymbol{w}_k^{(v)} \right| \leq \left| \boldsymbol{h}_{d,k}^H \right| + \sum_{n=1}^{N} \left| f_{n,k}^* \boldsymbol{g}_n^H \boldsymbol{w}_k^{(v)} \right|, \tag{4.36}$$

We allocate ℓ_m IRS elements to the mi-th UE using the BS-IRS-UE channel beamforming gain $\left| f_{n,m_i}^* \boldsymbol{g}_n^H \boldsymbol{w}_{m_i} \right|$ as the metric.
Thus, the allocation of a single IRS element can be done as follows

$$\begin{aligned} n_0 &= argmax_n \left| f_{n,m_i}^* \boldsymbol{g}_n^H \boldsymbol{w}_{m_i} \right|, n \in \mathcal{N}_0, \\ \mathcal{N}_{m_i} &= \mathcal{N}_{m_i} + \{n_0\},\ \mathcal{N}_0 = \mathcal{N}_0 - \{n_0\}. \end{aligned} \tag{4.37}$$

After allocating the IRS elements these IRS element phases will be updated and transmit beamformer updated and then they are performed.

4.4 Maximize Capacity for Multi-Users with 2 IRS's

In this model, we will use 2 IRS's, IRS1, IRS2, with N_1 and N_2 elements respectively, as shown in Fig. 4.3. Signals reflected by IRS more than once will

be disregarded because their power will be negligible compared to the path loss and the reflection power loss. In this case we have

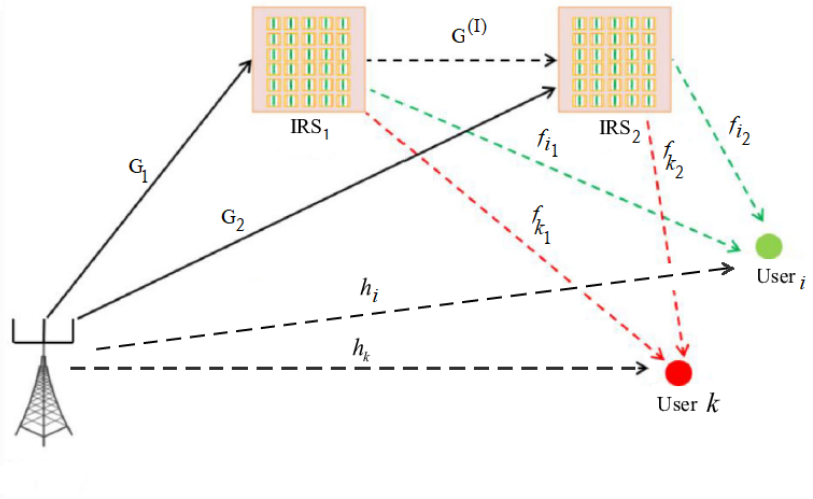

Figure 4.3: MISO model-assisted 2 IRS's without direct links between BS and UE and the I-SSR channel is considered.

$$\boldsymbol{H}_t = \boldsymbol{H} + \boldsymbol{F}^{(1)}\boldsymbol{\Phi}^{(\mathbf{1})}\boldsymbol{G}^{(1)H} + \boldsymbol{F}^{(2)}\boldsymbol{\Phi}^{(\mathbf{2})}\boldsymbol{G}^{(2)H}, \tag{4.38}$$

where $\boldsymbol{F}^{(1)}$ and $\boldsymbol{F}^{(2)}$ are defined as $\boldsymbol{F}$ for IRS1 and IRS2, respectively, $\boldsymbol{\Phi}^{(\mathbf{1})}$ and $\boldsymbol{\Phi}^{(\mathbf{2})}$ are reflection coefficient matrices of the 2 IRS's, also $\boldsymbol{G}^{(1)}$ and $\boldsymbol{G}^{(2)}$ are defined as $\boldsymbol{G}$ for the 2 IRS's. The received signal of UE k is

$$\begin{aligned} y_k = {} & [\boldsymbol{f}_k^{(1)H}\boldsymbol{\Phi}^{(\mathbf{1})}\boldsymbol{G}^{(1)H} + \boldsymbol{f}_k^{(2)H}\boldsymbol{\Phi}^{(\mathbf{2})}\boldsymbol{G}^{(2)H} + \boldsymbol{f}_k^{(2)H}\boldsymbol{\Phi}^{(\mathbf{2})}\boldsymbol{G}^{(I)H}\boldsymbol{\Phi}^{(\mathbf{1})}\boldsymbol{G}^{(1)H} + \boldsymbol{h}_k^H]\boldsymbol{x}_k \\ & + [\boldsymbol{f}_k^{(1)H}\boldsymbol{\Phi}^{(\mathbf{1})}\boldsymbol{G}^{(1)H} + \boldsymbol{f}_k^{(2)H}\boldsymbol{\Phi}^{(\mathbf{2})}\boldsymbol{G}^{(2)H} + \boldsymbol{f}_k^{(2)H}\boldsymbol{\Phi}^{(\mathbf{2})}\boldsymbol{G}^{(I)H}\boldsymbol{\Phi}^{(\mathbf{1})}\boldsymbol{G}^{(1)H} + \boldsymbol{h}_k^H]\sum_{i=1,i\neq k}^{K}\boldsymbol{x}_i + n_k, \end{aligned} \tag{4.39}$$

If the inter-surface signal reflection (I-SSR) has been ignored so that no cooperation exists between the 2 IRS's, then the $\boldsymbol{G}^{(I)}$ will be zero and (4.38) can be rewritten as follows

$$\begin{aligned} y_k = {} & [\boldsymbol{f}_k^{(1)H}\boldsymbol{\Phi}^{(\mathbf{1})}\boldsymbol{G}^{(1)H} + \boldsymbol{f}_k^{(2)H}\boldsymbol{\Phi}^{(\mathbf{2})}\boldsymbol{G}^{(2)H} + \boldsymbol{h}_k^H]\boldsymbol{x}_k \\ & + [\boldsymbol{f}_k^{(1)H}\boldsymbol{\Phi}^{(\mathbf{1})}\boldsymbol{G}^{(1)H} + \boldsymbol{f}_k^{(2)H}\boldsymbol{\Phi}^{(\mathbf{2})}\boldsymbol{G}^{(2)H} + \boldsymbol{h}_k^H]\sum_{i=1,i\neq k}^{K}\boldsymbol{x}_i + n_k, \end{aligned} \tag{4.40}$$

Or equivalently

$$\boldsymbol{y}_k = (\boldsymbol{H} + \boldsymbol{F}^{(1)}\boldsymbol{\Phi}^{(1)}\boldsymbol{G}^{(1)H} + \boldsymbol{F}^{(2)}\boldsymbol{\Phi}^{(2)}\boldsymbol{G}^{(2)H})\,\boldsymbol{W}\,\boldsymbol{s} + \boldsymbol{n}_k, \tag{4.41}$$

The I-SSR channel $\boldsymbol{G}^{(I)}$ was eliminated so without it we can design a single IRS instead of 2 IRS's, so the objective function can be manipulated in which the variable $\boldsymbol{\Phi}^{(1)}$ and $\boldsymbol{\Phi}^{(2)}$ are merged into a single matrix

$$\boldsymbol{H}_t = \boldsymbol{H} + \begin{bmatrix} \boldsymbol{F}^{(1)} & \boldsymbol{F}^{(2)} \end{bmatrix} \begin{bmatrix} \boldsymbol{\Phi}^{(1)} & 0 \\ 0 & \boldsymbol{\Phi}^{(2)} \end{bmatrix} \begin{bmatrix} \boldsymbol{G}^{(1)H} \\ \boldsymbol{G}^{(2)H} \end{bmatrix}$$

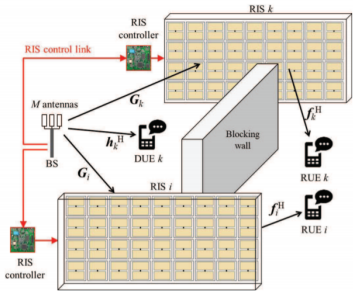

Figure 4.4: MISO model-assisted 2 IRS's with different link for each UE.

4.5 Numerical Results:

This section for the experiment part results, where we are using a fixed number of antennas at the base station, and the number of IRS elements (N) and the number of users (K) are changing.

4.5.1 One IRS

Fig. 4.5 shows the total capacity as a function of the signal to noise ratio (SNR) which is defined as the ratio of the transmit power to the power of the noise $\frac{P_t}{{\sigma_w}^2}$, where P_t is the transmitted power and ${\sigma_w}^2$ is the variance (The noise has expected value of zero). We have $K = 5$ users, the number of antennas at the Base Station is $M = 40$, the number of IRS elements N changes, and the fading

gain β is exponential distributed. The constant variables are c the speed of light, $\lambda = \frac{c}{f_c}$, where f_c is the cut-off frequency, the distance $d = \frac{\lambda}{2}$, and wave number $k = \frac{2\pi}{\lambda}$.
In the simulation we have $d_{IRS} = \frac{\lambda}{2}$, and $d_{BS} = \frac{\lambda}{2}$, and we considered the following solutions:
A. The First Model: We consider an IRS-aided downlink MISO system, where K single-antenna users and an IRS is deployed to enhance the communication performance. The BS is equipped with a uniform linear array (ULA) with M antennas, and the IRS is modeled as an planar array (UPA) which contains $N = N_y N_z$ passive reflecting elements. Assuming that CSI is known, water-filling will be used to optimize the power.
B. Comparing The First Model With The Algorithm 1 (GA) : We consider an IRS-aided downlink MISO system, where K single-antenna users and an IRS is deployed to enhance the communication performance. The BS is equipped with an ULA with M antennas, and the IRS is modeled as an UPA which contains $N = N_y N_z$ passive reflecting elements. We will use the algorithm 1 to optimize the phases and compare it with the first model.
Water-filling will be used to optimize the power.
C. Algorithm 1 (GA): We consider an IRS-aided downlink MISO system, where K single-antenna users and an IRS is deployed to enhance the communication performance. The BS is equipped with an ULA with M antennas, and the IRS is modeled as an UPA which contains $N = N_y N_z$ passive reflecting elements.
To increase the signal power at the intended user and reduce interference to non-intended users, the signal components should add destructively at non-intended users and that will happen by choosing the optimal phases. It is difficult to strike a perfect balance between maximizing the signal power and minimizing the interference leakage. In fact, the optimal beamforming is computed as a sequence of convex optimization problems, which are implemented and solved using algorithm 1 (ga Matlab function).
Water-filling will be used to optimize the power and we will redo it by eliminating the zero-power users and repeating the water-filling until there are no zero-power users.
D. Algorithm 2 (Alternating Beamforming Technique): We will use the same parameters of solution B. The optimal beamforming is computed as a sequence of convex optimization problems, which are implemented and solved using algorithm 2.
Water-filling will be used to optimize the power and we will redo it by eliminating the zero-power users and repeating the water-filling until there are no zero-power users.
E. Merging 2 IRSs As One IRS: We will use the same parameters as in A and B. We will use 2 IRSs, First we will use an algorithm to merge the 2 IRSs as one IRS by following the equations (4.38)-(4.41), then algorithm 2 is used to optimize the phases.
Water-filling will be used to optimize the power and we will redo it by elimi-

Table 4.2: The Number of Active Users for Different Number of IRS Elements

Number of IRS Elements	Number of Users / Number of Active Users									
$N = 36$	1/2	2/2	3/3	4/4	5/5	6/6	7/6	8/6	9/6	10/7
$N = 49$	1/2	2/2	3/3	4/4	5/5	6/6	7/6	8/6	9/7	10/8
$N = 64$	1/2	2/2	3/3	4/4	5/5	6/6	7/6	8/6	9/7	10/8
$N = 81$	1/2	2/2	3/3	4/4	5/5	6/6	7/6	8/7	9/7	10/8
$N = 100$	1/2	2/2	3/3	4/4	5/5	6/6	7/6	8/7	9/7	10/8

nating the zero-power users and repeating the water-filling until there are no zero-power users.

F. 2 IRSs Working Separately: We will also use the same parameters as in A and B. We will use 2 IRSs separately, then we will do the same steps in (D) from water-filling to using algorithm 2.

Fig. 4.6 shows the results for the solutions (a) while Fig. 4.8 shows the results when we implemented the solutions (c) and after using the algorithm and from Table 4.2 we can see the number of active users that we got after eliminating the users with zero power and redoing the water-filling and we repeat that for different numbers of IRS elements.

After (4.37) we will iterate the sequence iteratively V times, and we will have the results are shown in Fig. 4.10 where the capacity increases with the number of users and in Fig. 4.11 we can see the capacity with the number of the IRS elements. V to denote the v-th update of beamformer and IRS phases, $\boldsymbol{G} = [\boldsymbol{g}_1, \boldsymbol{g}_2, ..., \boldsymbol{g}_N] \in \mathbb{C}^{M \times N}$ is the channel from the BS to the IRS where $\boldsymbol{g}_n$ denotes the channel between the BS and the n-th IRS element.

4.5.2 Two IRSs

The results for 2 IRS's can be seen in Fig. 4.12, where the capacity increases with the number of users and in Fig. 4.13 the capacity increases with the number of IRS elements which in this case twice the number of elements in one IRS if we consider that both IRS's have the same number of elements. Also in our scenario, we are using the water-filling to optimize the power and algorithm 2 to optimize the phase shifters at the IRS.

It is not required for the same user to have a direct connection as well as a link reflected from one of the IRS's. We can have a user with a direct link, and the other users have the reflected links from the IRS's only. From the Fig. 4.4, there are two IRS's, and in this scenario, each IRS serves a group of users individually

(the two IRS's are not combined as one large IRS). The results are shown in Fig. 4.14 and Fig. 4.15.

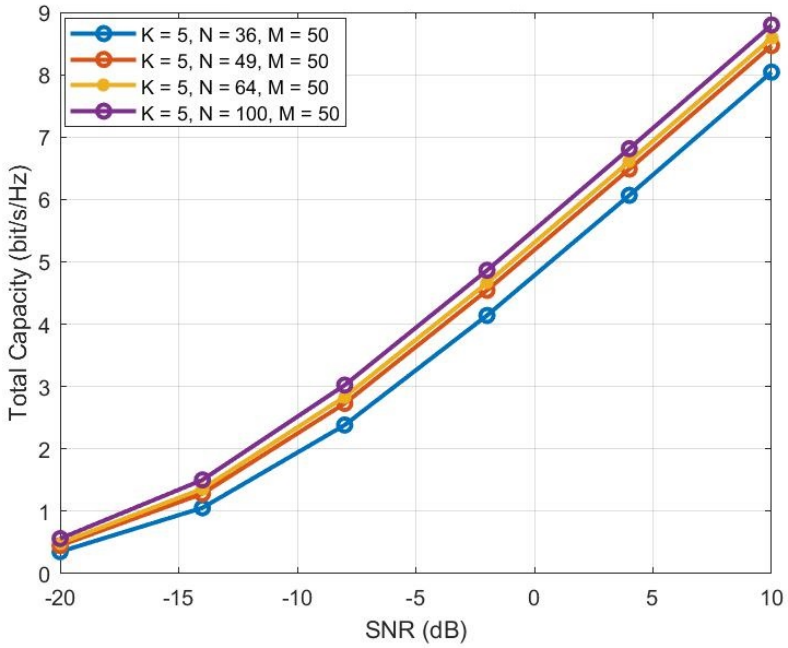

Figure 4.5: Total capacity as a function of the SNR, for K=5 Users, M=40 antennas of the BS, and the various number of IRS elements N. As the SNR increases the total capacity increases.

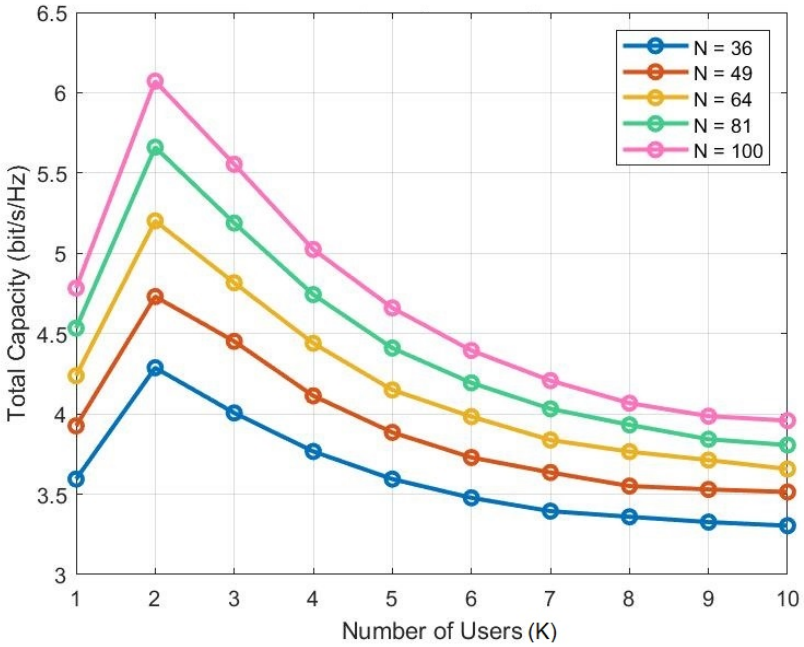

Figure 4.6: The solutions (a): Total capacity as a function of the number of users K, and the number of IRS elements N, with M=40 antennas of the BS. As K increases the total capacity increases until K=2 then start decreasing, also, the total capacity increases with N.

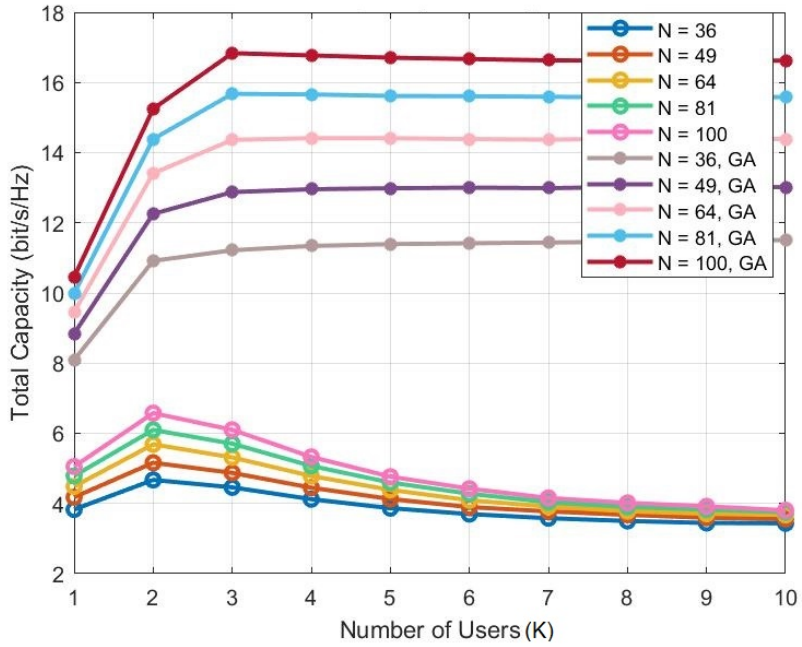

Figure 4.7: The solutions (b): Total capacity as a function of the number of users K, and the number of IRS elements N, with M=40 antennas of the BS. As K increases the total capacity increases for the First Model until K=2 then starts decreasing, while with the Algorithm 1 the total capacity increases until K=3 then start decreasing, also in both cases, the total capacity increases with N.

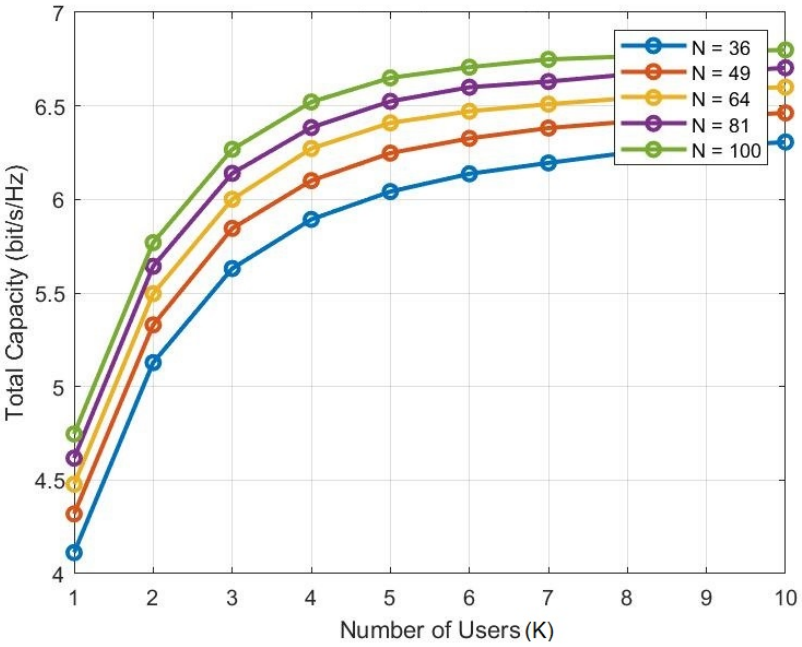

Figure 4.8: The solutions (c): Total capacity as a function of the number of users K, and the number of IRS elements N, with M=40 antennas of the BS. Interference obtained with Algorithm 1. As the K increases the total capacity increases.

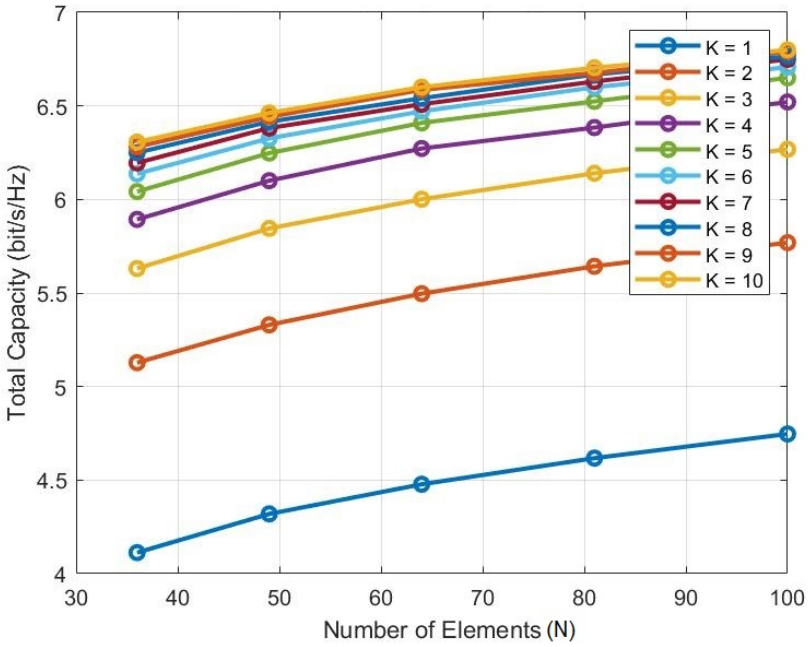

Figure 4.9: The solutions (c): Total capacity as a function of the and number of IRS elements N, and the number of users K, with M=40 antennas of the BS. Interference obtained with Algorithm 1. As N increases the total capacity increases.

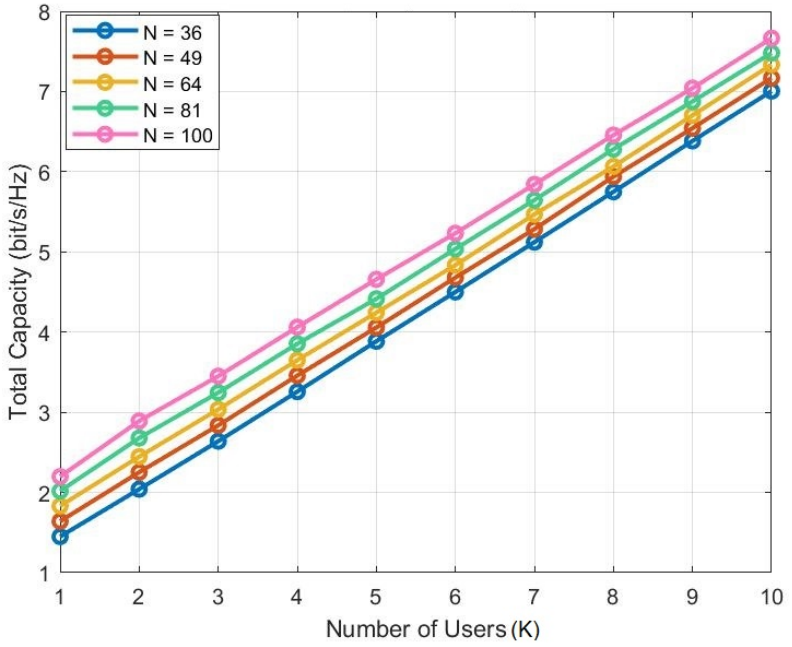

Figure 4.10: The solutions (d): Total capacity as a function of the number of users K, and the number of IRS elements N, with M=40 antennas of the BS. Interference obtained with Algorithm 2. As K increases the total capacity increases.

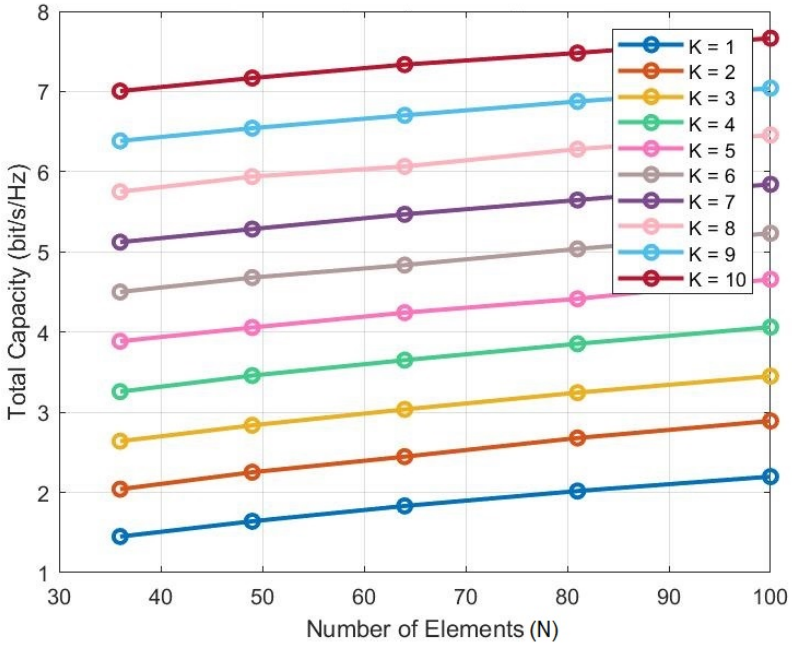

Figure 4.11: The solutions (d): Total capacity as a function of the number of IRS elements N, and the number of users K, with M=40 antennas of the BS. Interference obtained with Algorithm 2. As N increases the total capacity increases.

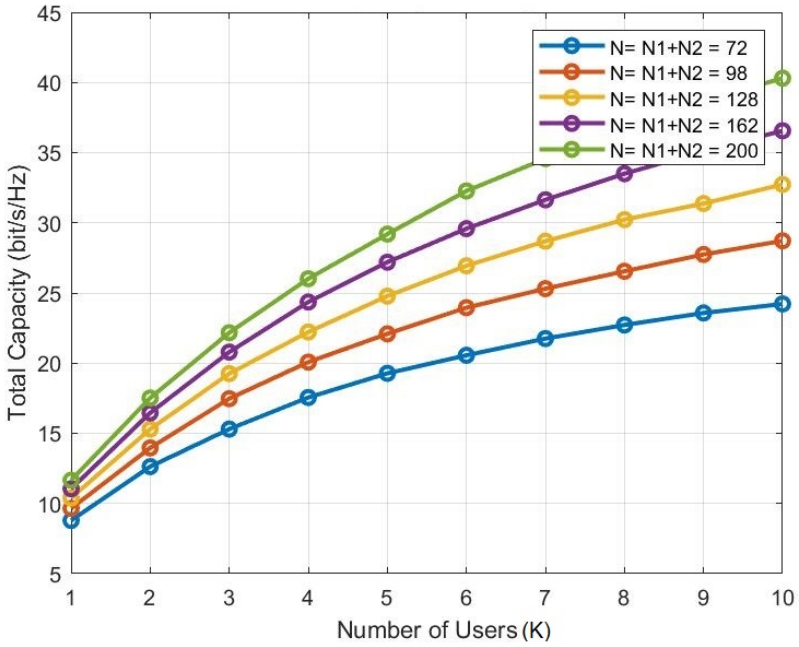

Figure 4.12: The solutions (e): Total capacity as a function of the number of users K, and the number of IRS elements N, with M=40 antennas of the BS. The 2 IRSs merged as one IRS. As K increases the total capacity increases.

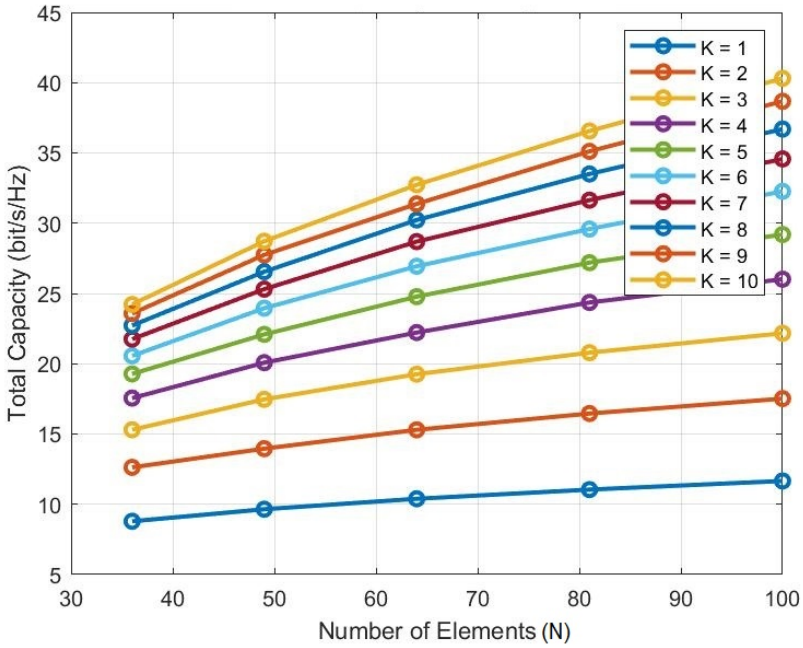

Figure 4.13: The solutions (e): Total capacity as a function of the number of IRS elements N, and the number of users K, with M=40 antennas of the BS. The 2 IRSs merged as one IRS. As N increases the total capacity increases.

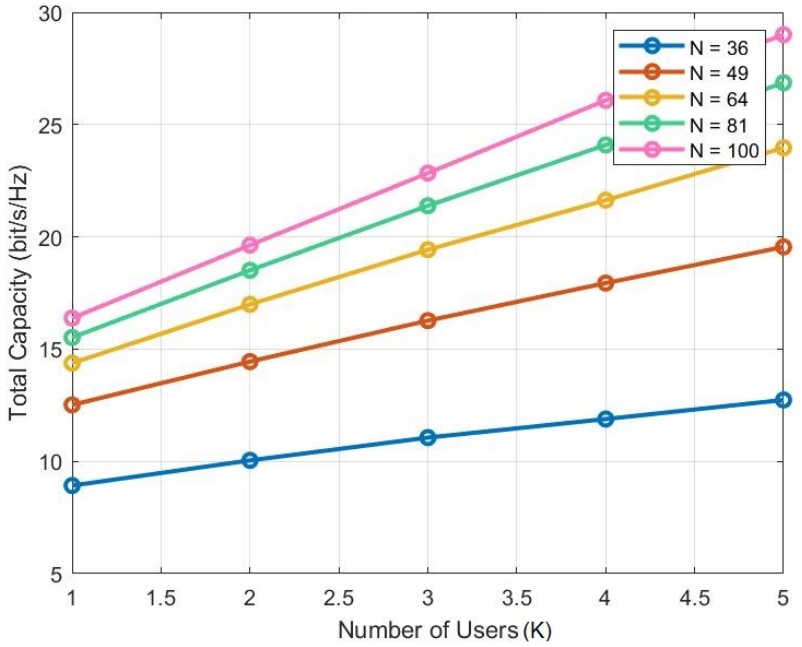

Figure 4.14: The solutions (f): Total capacity as a function of the number of users K, and the number of IRS elements N, with M=40 antennas of the BS. Each one of the 2 IRSs works separately on the other. As K increases the total capacity increases.

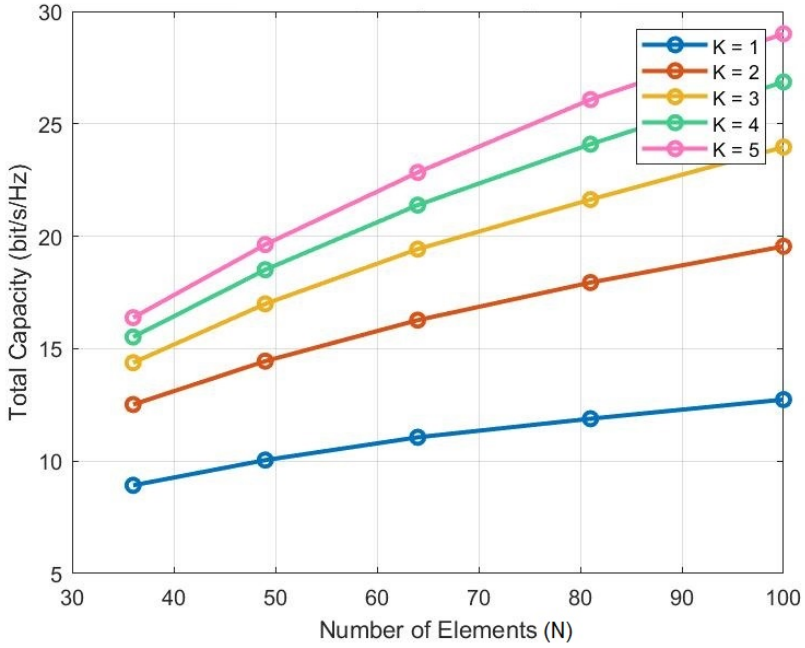

Figure 4.15: The solutions (f): Total capacity as a function of the number of IRS elements N, and the number of users K, with M=40 antennas of the BS. Each one of the 2 IRSs works separately on the other. As N increases the total capacity increases.

Chapter 5

Conclusion

This thesis analyzed the downlink optimization scenario for IRSs and solved the capacity maximization problem for MISO-assisted IRS communication. The network scheduling or resource allocation problem can be solved by optimizing power and phases and mitigating interference between users. We also assume that the CSI is already known.
We used the water-filling algorithm to optimize the power, while the GA and an alternating beamforming technique were used to optimize the phases, and the results of these two algorithms are that the total capacity of the system is increased when neither the number of users nor the number of elements increases. According to the numerical results, our proposed algorithms GA and the alternating beamforming technique improved the performance of the system and increased its capacity compared to that of the system without these algorithms. Also, the results of algorithm 2 show slightly better results than algorithm 1 in term of the total capacity.
The results with two IRSs show that the capacity of the IRS aided by the MISO system can be significantly improved by increasing the number of IRS.

Bibliography

[1] Ertugrul Basar, Marco Di Renzo, Julien De Rosny, Merouane Debbah, Mohamed-Slim Alouini, and Rui Zhang. Wireless communications through reconfigurable intelligent surfaces. *IEEE Access*, 7:116753–116773, 2019.

[2] Ludek Subrt and Pavel Pechac. Controlling propagation environments using intelligent walls. In *2012 6th European Conference on Antennas and Propagation (EUCAP)*, pages 1–5, 2012.

[3] Nadège Kaina, Matthieu Dupré, Geoffroy Lerosey, and Mathias Fink. Shaping complex microwave fields in reverberating media with binary tunable metasurfaces. *Scientific Reports*, 4, 2014.

[4] Tie Jun Cui, Mei Qing Qi, Xiang Wan, Jie Zhao, and Qiang Cheng. Coding metamaterials, digital metamaterials and programming metamaterials, 2014.

[5] H Yang, X Cao, F Yang, J Gao, S Xu, M Li, X Chen, Y Zhao, Y Zheng, and S Li. A programmable metasurface with dynamic polarization, scattering and focusing control. *Scientific Reports*, 6, 2016.

[6] Xin Tan, Zhi Sun, Josep M. Jornet, and Dimitris Pados. Increasing indoor spectrum sharing capacity using smart reflect-array. In *2016 IEEE International Conference on Communications (ICC)*, pages 1–6, 2016.

[7] Sha Hu, Fredrik Rusek, and Ove Edfors. The potential of using large antenna arrays on intelligent surfaces. *CoRR*, abs/1702.03128, 2017.

[8] L Christos, N Shuai, T Ageliki, P Andreas, I Sotiris, and A Ian F. A novel communication paradigm for high capacity and security via programmable indoor wireless environments in next generation wireless systems. *CoRR*, abs/1812.07096, 2018.

[9] Luca Sanguinetti, Emil Björnson, and Jakob Hoydis. Toward massive mimo 2.0: Understanding spatial correlation, interference suppression, and pilot contamination. *IEEE Transactions on Communications*, 68(1):232–257, 2020.

[10] Ish Kumar Jain, Rajeev Kumar, and Shivendra S. Panwar. The impact of mobile blockers on millimeter wave cellular systems. *IEEE Journal on Selected Areas in Communications*, 37(4):854–868, 2019.

[11] Jiayi Zhang, Linglong Dai, Xu Li, Ying Liu, and Lajos Hanzo. On low-resolution adcs in practical 5g millimeter-wave massive mimo systems. *IEEE Communications Magazine*, 56(7):205–211, 2018.

[12] Wan Choi and Jeffrey G. Andrews. Downlink performance and capacity of distributed antenna systems in a multicell environment. *IEEE Transactions on Wireless Communications*, 6(1):69–73, 2007.

[13] Jun Zhang, Runhua Chen, Jeffrey G. Andrews, Arunabha Ghosh, and Robert W. Heath. Networked mimo with clustered linear precoding. *IEEE Transactions on Wireless Communications*, 8(4):1910–1921, 2009.

[14] Hoon Huh, Antonia M. Tulino, and Giuseppe Caire. Network mimo with linear zero-forcing beamforming: Large system analysis, impact of channel estimation, and reduced-complexity scheduling. *IEEE Transactions on Information Theory*, 58(5):2911–2934, 2012.

[15] Hengtao He, Xianghao Yu, Jun Zhang, S. H. Song, and Khaled B. Letaief. Cell-free massive MIMO for 6g wireless communication networks. *CoRR*, abs/2110.07309, 2021.

[16] Elina Nayebi, Alexei Ashikhmin, Thomas L. Marzetta, Hong Yang, and Bhaskar D. Rao. Precoding and power optimization in cell-free massive mimo systems. *IEEE Transactions on Wireless Communications*, 16(7):4445–4459, 2017.

[17] Mugen Peng, Yaohua Sun, Xuelong Li, Zhendong Mao, and Chonggang Wang. Recent advances in cloud radio access networks: System architectures, key techniques, and open issues. *IEEE Communications Surveys Tutorials*, 18(3):2282–2308, 2016.

[18] Giovanni Interdonato, Emil Björnson, Hien Quoc Ngo, Pål K. Frenger, and Erik G. Larsson. Ubiquitous cell-free massive MIMO communications. *CoRR*, abs/1804.03421, 2018.

[19] M. I. Skolnik. *Introduction to Radar Systems*. McGRAW-HILL. New york, USA, 2001.

[20] Jiayi Zhang, Emil Björnson, Michail Matthaiou, Derrick Wing Kwan Ng, Hong Yang, and David J. Love. Prospective multiple antenna technologies for beyond 5g. *IEEE Journal on Selected Areas in Communications*, 38(8):1637–1660, 2020.

[21] Omar El Ayach, Sridhar Rajagopal, Shadi Abu-Surra, Zhouyue Pi, and Robert W. Heath. Spatially sparse precoding in millimeter wave mimo systems. *IEEE Transactions on Wireless Communications*, 13(3):1499–1513, 2014.

[22] Marco Di Renzo, Alessio Zappone, Merouane Debbah, Mohamed-Slim Alouini, Chau Yuen, Julien de Rosny, and Sergei Tretyakov. Smart radio environments empowered by reconfigurable intelligent surfaces: How it works, state of research, and the road ahead. *IEEE Journal on Selected Areas in Communications*, 38(11):2450–2525, 2020.

[23] Mikko Heino, Dani Korpi, Timo Huusari, Emilio Antonio-Rodriguez, Sathya Venkatasubramanian, Taneli Riihonen, Lauri Anttila, Clemens Icheln, Katsuyuki Haneda, Risto Wichman, and Mikko Valkama. Recent advances in antenna design and interference cancellation algorithms for in-band full duplex relays. *IEEE Communications Magazine*, 53(5):91–101, 2015.

[24] Chongwen Huang, Alessio Zappone, George C. Alexandropoulos, Mérouane Debbah, and Chau Yuen. Reconfigurable intelligent surfaces for energy efficiency in wireless communication. *IEEE Transactions on Wireless Communications*, 18(8):4157–4170, 2019.

[25] Emil Björnson, Özgecan Özdogan, and Erik G. Larsson. Reconfigurable intelligent surfaces: Three myths and two critical questions. *IEEE Communications Magazine*, 58(12):90–96, 2020.

[26] Qingqing Wu and Rui Zhang. Towards smart and reconfigurable environment: Intelligent reflecting surface aided wireless network. *IEEE Communications Magazine*, 58(1):106–112, 2020.

[27] Emil Björnson and Luca Sanguinetti. Power scaling laws and near-field behaviors of massive MIMO and intelligent reflecting surfaces. *CoRR*, abs/2002.04960, 2020.

[28] O Tsilipakos. *Toward Intelligent Metasurfaces: The Progress from Globally Tunable Metasurfaces to Software-Defined Metasurfaces with an Embedded Network of Controllers*. Advanced Optical Materials, 2020.

[29] Özgecan Özdogan, Emil Björnson, and Erik G. Larsson. Intelligent reflecting surfaces: Physics, propagation, and pathloss modeling. *IEEE Wireless Communications Letters*, 9(5):581–585, 2020.

[30] Jian Dang, Zaichen Zhang, and Liang Wu. Joint beamforming for intelligent reflecting surface aided wireless communication using statistical csi. *China Communications*, 17(8):147–157, 2020.

[31] Zheng Chu, Pei Xiao, De Mi, Hongzhi Chen, and Wanming Hao. Intelligent reflecting surfaces enabled cognitive internet of things based on practical pathloss model. *China Communications*, 17(12):1–16, 2020.

[32] Zijie Ji, Phee Lep Yeoh, Deyou Zhang, Gaojie Chen, Yan Zhang, Zunwen He, Hao Yin, and Yonghui li. Secret key generation for intelligent reflecting surface assisted wireless communication networks. *IEEE Transactions on Vehicular Technology*, 70(1):1030–1034, 2021.

[33] Yunchuan Wei, Kai Zeng, and Prasant Mohapatra. Adaptive wireless channel probing for shared key generation based on pid controller. *IEEE Transactions on Mobile Computing*, 12(9):1842–1852, 2013.

[34] Neal Patwari, Jessica Croft, Suman Jana, and Sneha K. Kasera. High-rate uncorrelated bit extraction for shared secret key generation from channel measurements. *IEEE Transactions on Mobile Computing*, 9(1):17–30, 2010.

[35] Dajiang Chen, Zhen Qin, Xufei Mao, Panlong Yang, Zhiguang Qin, and Ruijin Wang. Smokegrenade: An efficient key generation protocol with artificial interference. *IEEE Transactions on Information Forensics and Security*, 8(11):1731–1745, 2013.

[36] Shengnan Wang and Chunguang Li. Discrete double-bit hashing. *IEEE Transactions on Big Data*, pages 1–1, 2019.

[37] Beixiong Zheng and Rui Zhang. Intelligent reflecting surface-enhanced ofdm: Channel estimation and reflection optimization. *IEEE Wireless Communications Letters*, 9(4):518–522, 2020.

[38] Abdelrahman Taha, Muhammad Alrabeiah, and Ahmed Alkhateeb. Deep learning for large intelligent surfaces in millimeter wave and massive mimo systems. In *2019 IEEE Global Communications Conference (GLOBECOM)*, pages 1–6, 2019.

[39] George C. Alexandropoulos and Evangelos Vlachos. A hardware architecture for reconfigurable intelligent surfaces with minimal active elements for explicit channel estimation. In *ICASSP 2020 - 2020 IEEE International Conference on Acoustics, Speech and Signal Processing (ICASSP)*, pages 9175–9179, 2020.

[40] Zhaorui Wang, Liang Liu, and Shuguang Cui. Channel estimation for intelligent reflecting surface assisted multiuser communications: Framework, algorithms, and analysis. *CoRR*, abs/1912.11783, 2019.

[41] Chongwen Huang, Sha Hu, George C. Alexandropoulos, Alessio Zappone, Chau Yuen, Rui Zhang, Marco Di Renzo, and Merouane Debbah. Holographic mimo surfaces for 6g wireless networks: Opportunities, challenges, and trends. *IEEE Wireless Communications*, 27(5):118–125, 2020.

[42] Arthur S. de Sena, Dick Carrillo, Fang Fang, Pedro H. J. Nardelli, Daniel B. da Costa, Ugo S. Dias, Zhiguo Ding, Constantinos B. Papadias, and Walid Saad. What role do intelligent reflecting surfaces play in multi-antenna non-orthogonal multiple access? *IEEE Wireless Communications*, 27(5):24–31, 2020.

[43] Senglee Foo. Liquid-crystal-tunable metasurface antennas. In *2017 11th European Conference on Antennas and Propagation (EUCAP)*, pages 3026–3030, 2017.

[44] Chongwen Huang, George C. Alexandropoulos, Alessio Zappone, Mérouane Debbah, and Chau Yuen. Energy efficient multi-user MISO communication using low resolution large intelligent surfaces. *CoRR*, abs/1809.05397, 2018.

[45] Chongwen Huang, Alessio Zappone, Mérouane Debbah, and Chau Yuen. Achievable rate maximization by passive intelligent mirrors. *CoRR*, abs/1807.07196, 2018.

[46] Qingqing Wu and Rui Zhang. Intelligent reflecting surface enhanced wireless network: Joint active and passive beamforming design. *CoRR*, abs/1809.01423, 2018.

[47] Qingqing Wu and Rui Zhang. Beamforming optimization for intelligent reflecting surface with discrete phase shifts. In *ICASSP 2019 - 2019 IEEE International Conference on Acoustics, Speech and Signal Processing (ICASSP)*, pages 7830–7833, 2019.

[48] Ertugrul Basar. Transmission through large intelligent surfaces: A new frontier in wireless communications, 2019.

[49] Qurrat-Ul-Ain Nadeem, Abla Kammoun, Anas Chaaban, Mérouane Debbah, and Mohamed-Slim Alouini. Asymptotic analysis of large intelligent surface assisted MIMO communication. *CoRR*, abs/1903.08127, 2019.

[50] Xianghao Yu, Dongfang Xu, and Robert Schober. Miso wireless communication systems via intelligent reflecting surfaces : (invited paper). In *2019 IEEE/CIC International Conference on Communications in China (ICCC)*, pages 735–740, 2019.

[51] Yu Han, Wankai Tang, Shi Jin, Chao-Kai Wen, and Xiaoli Ma. Large intelligent surface-assisted wireless communication exploiting statistical csi. *IEEE Transactions on Vehicular Technology*, 68(8):8238–8242, 2019.

[52] Deepak Mishra and Håkan Johansson. Channel estimation and low-complexity beamforming design for passive intelligent surface assisted miso wireless energy transfer. In *ICASSP 2019 - 2019 IEEE International Conference on Acoustics, Speech and Signal Processing (ICASSP)*, pages 4659–4663, 2019.

[53] Abdelrahman Taha, Muhammad Alrabeiah, and Ahmed Alkhateeb. Enabling large intelligent surfaces with compressive sensing and deep learning. *CoRR*, abs/1904.10136, 2019.

[54] Zhen-Qing He and Xiaojun Yuan. Cascaded channel estimation for large intelligent metasurface assisted massive mimo. *IEEE Wireless Communications Letters*, 9(2):210–214, 2020.

[55] Xianghao Yu, Dongfang Xu, and Robert Schober. Enabling secure wireless communications via intelligent reflecting surfaces. In *2019 IEEE Global Communications Conference (GLOBECOM)*, pages 1–6, 2019.

[56] Jie Chen, Ying-Chang Liang, Yiyang Pei, and Huayan Guo. Intelligent reflecting surface: A programmable wireless environment for physical layer security. *IEEE Access*, 7:82599–82612, 2019.

[57] Haiquan Lu, Yong Zeng, Shi Jin, and Rui Zhang. Enabling panoramic full-angle reflection via aerial intelligent reflecting surface. In *2020 IEEE International Conference on Communications Workshops (ICC Workshops)*, pages 1–6, 2020.

[58] Sha Hu, Fredrik Rusek, and Ove Edfors. Beyond massive mimo: The potential of data transmission with large intelligent surfaces. *IEEE Transactions on Signal Processing*, 66(10):2746–2758, 2018.

[59] Christos Liaskos, Ageliki Tsioliaridou, Shuai Nie, Andreas Pitsillides, Sotiris Ioannidis, and Ian Akyildiz. An interpretable neural network for configuring programmable wireless environments. In *2019 IEEE 20th International Workshop on Signal Processing Advances in Wireless Communications (SPAWC)*, pages 1–5, 2019.

[60] Miao Cui, Guangchi Zhang, and Rui Zhang. Secure wireless communication via intelligent reflecting surface. *IEEE Wireless Communications Letters*, 8(5):1410–1414, 2019.

[61] Sha Hu, Fredrik Rusek, and Ove Edfors. Cramér-rao lower bounds for positioning with large intelligent surfaces. In *2017 IEEE 86th Vehicular Technology Conference (VTC-Fall)*, pages 1–6, 2017.

[62] Minchae Jung, Walid Saad, Youngrok Jang, Gyuyeol Kong, and Sooyong Choi. Performance analysis of large intelligent surfaces (liss): Asymptotic data rate and channel hardening effects. *IEEE Transactions on Wireless Communications*, 19(3):2052–2065, 2020.

[63] Ertugrul Basar. Reconfigurable intelligent surface-based index modulation: A new beyond mimo paradigm for 6g. *IEEE Transactions on Communications*, 68(5):3187–3196, 2020.

[64] Junyi Wang, Zhou Lan, Chang woo Pyo, T. Baykas, Chin sean Sum, M.A. Rahman, Jing Gao, R. Funada, F. Kojima, H. Harada, and S. Kato. Beam codebook based beamforming protocol for multi-gbps millimeter-wave wpan systems. *IEEE Journal on Selected Areas in Communications*, 27(8):1390–1399, 2009.

[65] Sooyoung Hur, Taejoon Kim, David J. Love, James V. Krogmeier, Timothy A. Thomas, and Amitava Ghosh. Millimeter wave beamforming for wireless backhaul and access in small cell networks. *IEEE Transactions on Communications*, 61(10):4391–4403, 2013.

[66] Ahmed Alkhateeb, Omar El Ayach, Geert Leus, and Robert W. Heath. Channel estimation and hybrid precoding for millimeter wave cellular systems. *IEEE Journal of Selected Topics in Signal Processing*, 8(5):831–846, 2014.

[67] Minchae Jung, Walid Saad, Mérouane Debbah, and Choong Seon Hong. On the optimality of reconfigurable intelligent surfaces (riss): Passive beamforming, modulation, and resource allocation. *IEEE Transactions on Wireless Communications*, 20(7):4347–4363, 2021.

[68] J. Carr. An introduction to genetic algorithms. 2014.

[69] Hyesang Cho and Junil Choi. Alternating beamforming with intelligent reflecting surface element allocation. *IEEE Wireless Communications Letters*, 10:1232–1236, 2021.